THEORETICAL PASSIVE EARTH PRESSURE COEFFICIENTS FOR A COHESIONLESS DRY SOIL BEHIND ROUGH VERTICAL WALLS

by

Ali Zeki Tolunay

Submitted in partial fulfillment
of the requirements for the degree of
Master of Applied Science

Department of Civil Engineering
School of Graduate Studies
University of Ottawa
Ottawa, Canada

January, 1972

To

the memory of my father

Prof. Dr. Mithat Ali Tolunay

PREFACE

The publishing of Charles Augustin Coulomb's work " Essai sur une application des règles de maximus et minimis à quelques problèmes de statique relatifs à l'architecture " in 1776 marked the first rigorous analysis of the lateral earth pressure problem. Coulomb's consideration of a sliding wedge behind a wall for the active (wall yielding away from the backfill) and for the passive (wall pushing against the backfill) cases gives useful results agreeing with the experimental values for the lateral pressures with no wall friction, ie. smooth wall. On the other hand his results differ considerably from reality when applied to a rough wall with the backfill in a passive state.

Following this work other analyses were introduced by various authors, such as : W. Rankine, H. Krey, J. Ohde, K. Terzaghi, A. Caquot, Brinch Hansen, V. Sokolovski, N. Janbu and P. Rowe, in order to estimate the lateral earth pressures on structures.

The principal contribution of the more recent workers was to alter the plane shape of Coulomb's failure wedge into the shape of a curved surface when there was wall friction present. Different authors used different shapes for this curved surface and calculated the lateral pressures accordingly. These studies showed that there was no appreciable disagreement between the values computed for the active case and the Coulomb's values, but the passive pressure values differed appreciably from Coulomb's calculations, in agreement with the experimental findings.

A careful experimental study of the passive earth pressure case for sands was carried out by K. Peaker in 1964 at the University of Manchester under professor P. Rowe. A rough wall gave values of passive earth pressure coefficients (ratio of the horizontal force to the vertical force at the wall, when the wall pushes towards the backfill) lower than the theoretical values available at that time. Since for many structures the passive earth pressure is relied upon at least partially for stability, Peaker's results were very disturbing. All existing theories gave predictions which were unsafe for rough walls.

Although Rowe had worked out a theory for the earth pressure problem using the method of slices commonly employed in slope stability work, only a limited number of calculations appears to have been made and no comparison was made with Peaker's results. In fact Rowe's theory is as yet unpublished except for a brief reference to the method in " Selected Topics in Soil Mechanics " edited by I. K. Lee. It is this method that is used in this study of the particular problem of a rough, vertical wall pushing into a cohesionless, dry backfill with a horizontal ground surface.

Passive earth pressure coefficients, K_p, based on

Rowe's method are presented for angles of internal friction, ϕ', varying from 20 degrees to 45 degrees (representing loose to dense sand) and for wall friction angles, δ, of zero degrees to ϕ' degrees (representing smooth to rough walls). These results are consistantly lower than those of previous theories and are quite close to the experimental values found by Peaker.

ACKNOWLEDGEMENTS

The author wishes to thank his supervisor, Dr. D. H. Shields, whose valuable guidance made this thesis possible.

Thanks are owed to the National Research Council of Canada for financial aid and to the Dean of the Faculty of Science and Engineering, Dr. A. D'Iorio, for the use of the facilities in the University.

Assistance was also received from the department of Civil Engineering and especially from the Chairman of the Department, Dr. J. D. Scott.

TABLE OF CONTENTS

LIST OF TABLES AND ILLUSTRATIONS

Figure		Page

Figure Page

NOTATION

a = distance from the center of a logarithmic spiral failure surface to the top of the wall.

b = slice width.

c = cohesion.

c' = effective cohesion.

c_e = effective cohesion with factor of safety.

dx = infinitesimal slice width.

dy_t = vertical distance between two normal forces on each side of a slice.

E = horizontal force on the slice.

E_b = summation of the horizontal forces on the slices, acting at the wall.

e = base of the Napierian logarithms.

F = factor of safety.

f = coefficient of friction.

H = height of wall.

H' = perpendicular distance from the center of logarithmic spiral failure surface to ground surface.

H_R = height on which Rankine state of stress acts.

h = height of slice.

h_t = distance from the bottom of a slice to the point of action of the normal force on the slice.

K_p = coefficient of passive earth pressure, normal to wall.

l = length.

N = force normal to the shearing surface.

N' = effective force normal to the shearing surface.

P = vertical external force.

P_p = passive earth force.

p_p = passive earth pressure.

P_R = passive earth force exerted by a mass in Rankine state.

Q = horizontal external force.

R = resultant of tangential and normal forces.

r = radius vector of a logarithmic spiral failure surface.

r_o = radius vector of a logarithmic spiral failure surface to the bottom of the wall.

r' = radius.

S = shearing force.

u = pore pressure.

W = weight.

x = horizontal distance.

X = shearing force on the side of a slice.

X_b = shearing force at the wall.

y = vertical distance.

α = the angle between the tangent to the failure surface and the horizontal.

α_t = $\arctan(dy_t/dx)$.

α_{tw} = α_t angle at the wall.

α_w = α angle at the wall.

γ = unit weight of soil.

$\Delta\theta$ = angle between two radius vectors of a logarithmic spiral failure surface determining the slice width.

δ = wall friction angle.

δ_e = wall friction angle with factor of safety.

θ = the angle between two radius vectors of a logarithmic failure surface.

θ_m = maximum value of θ.

π = 3.14159

ρ = inclination of the plane failure wedge to horizontal.

σ = normal stress.

σ' = effective normal stress.

σ_1 = major principal stress.

σ_3 = minor principal stress.

σ_h = horizontal normal stress.

σ_v = vertical normal stress.

τ = shearing stress.

τ_f = shearing stress with factor of safety.

ϕ = internal friction angle.

ϕ' = effective internal friction angle.

ϕ_e = internal friction angle with factor of safety.

Ψ = the angle between a radius vector and the tangent to the logarithmic spiral failure surface.

PART I. PREVIOUS WORK ON THE SUBJECT

CHAPTER 1. INTRODUCTION

CHAPTER 2. THEORETICAL REVIEW

CHAPTER 3. EXPERIMENTAL REVIEW

CHAPTER 1. INTRODUCTION

The passive earth pressure problem gained considerable understanding with the pioneering work of Coulomb in 1776. For the case of a rough wall acting against cohesionless backfill, Coulomb's theory gives passive earth pressure coefficient, K_p, values that are much higher than those given by the other more recent theories. All theories consider a failure surface of one shape or other and the location of the failure surface is critical to the results. It is necessary to find the location of the most critical surface by trial and error procedures.

After reviewing the more important theories in chapter 2, published experimental results are collected in chapter 3 and compared with these theories. Only the relatively simple case of a rough, rigid, vertical wall with horizontal backfill composed of cohesionless, dry sand is considered in this thesis.

Two theories, those of Janbu and Rowe, use the method of slices considering inter-slice forces. A detailed explanation of Janbu's slice method is given in chapter 4. Rowe's method of slices is outlined in chapter 5.

Values of K_p based on Rowe's method are computed and presented in chapter 6. The calculated values are compared with published experimental results and with the previous theories in chapter 7.

Definitions of the terms used frequently in the thesis are given below :

Earth pressure : the pressure exerted by soil on any boundary.

Active earth pressure, p_a : the minimum value of the horizontal earth pressure which can act on a vertical retaining wall. This condition exists when a soil mass is permitted to yield sufficiently to cause its internal shearing resistance along the potential failure surface to be completely mobilized.

Passive earth pressure, p_p : the maximum value of the horizontal earth pressure which can be created by a vertical retaining wall. This condition exists when a soil mass is compressed sufficiently to cause its internal shearing resistance along the potential failure surface to be completely mobilized.

Coefficient of earth pressure, K : the ratio of the horizontal to vertical pressures at a point in a soil mass.

Coefficient of passive earth pressure, K_p : the maximum value of K under passive pressure conditions.

Wall friction : frictional resistance mobilized between a wall and the soil in contact with it.

Angle of wall friction, δ : arctangent of the ratio of the shear force to the normal force at the wall. For the case of a vertical wall, the resultant passive force will make an angle of δ with the horizontal. The sign convention for δ is explained in the accompanying sketches.

δ positive $\qquad\qquad$ δ negative

Failure (rupture) surface : the surface within the soil mass on which simultaneous, plastic failure is assumed to be taking place.

CHAPTER 2. THEORETICAL REVIEW

Before Coulomb had published his paper on earth pressures in 1776 some French engineers had worked on this problem, but their work was not sufficiently cohesive to establish a theory. Among these engineers we can count : Marquis de Vauban, Bullet, Rondelet and Couplet (9).

Coulomb's theory is still useful in practice today and the earth pressure theories which followed this made use of his concepts whether the authors were aware of them or not. For these reasons Coulomb's earth pressure theory is discussed briefly here.

In his earth pressure theory Coulomb made the following assumptions (figure 1) :

The soil in question, which is behind the rigid retaining wall AB is ideal, ie. dry, homogenous, isotropic, elastically undeformable, granular, non-cohesive, resisting only compressive and shear stresses.

Coulomb assumed a wedge shaped failure mass ABC when the wall yields, and in the case of passive earth resistance, the wall pushing against the soil, the soil wedge is assumed to slide sideways and upward on the plane failure surface BC.

The rupture surface is assumed to pass through the heel of the wall, making an angle of ρ with the horizontal.

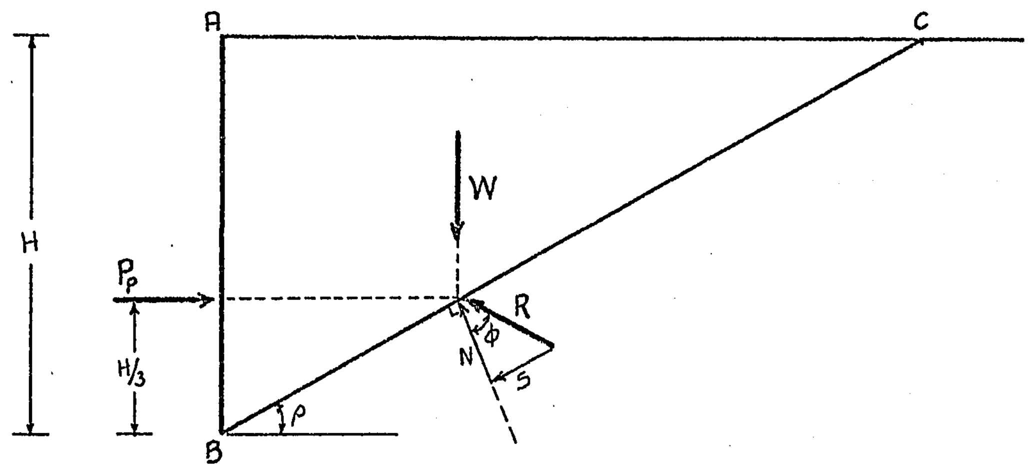

Figure 1. Coulomb's theory, $\delta=0$

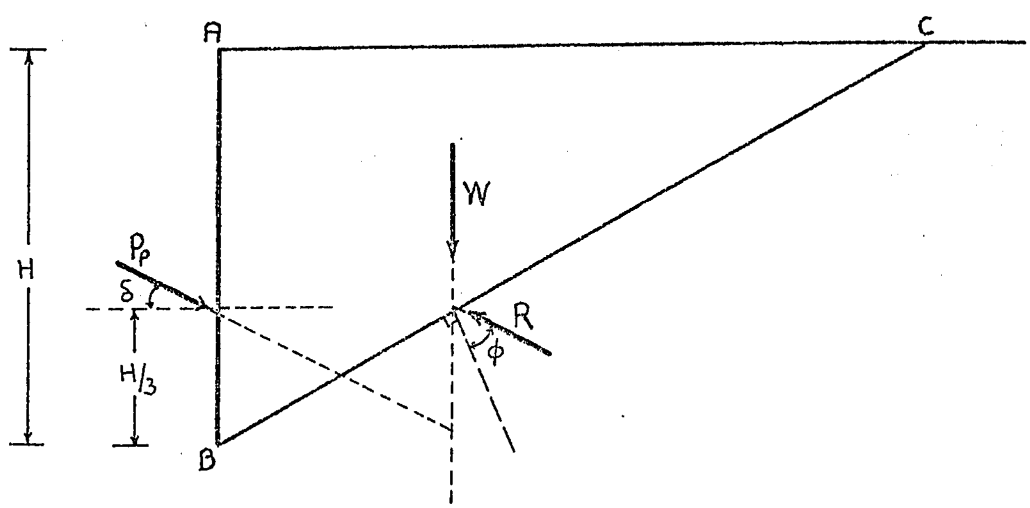

Figure 2. Coulomb's theory, $\delta>0$

The friction within the soil or in between the soil and the wall is represented by the classical law of Newton, which is stated as :

$$f = \tan\phi = \frac{S}{N} \qquad (2.1)$$

and being distributed evenly on the failure surface. This equation was written in the form :

$$\tau = \sigma.\tan\phi \qquad (2.2)$$

When there is equilibrium, the resultant force R makes an angle of ϕ with the normal to the failure surface. The position and direction of the passive force, P_p, is assumed to be known and Coulomb also assumed the angle of wall friction, δ, as zero. The solution is two dimensional, and a unit width of wall and soil is considered.

With these assumptions, in order to find the force exerted by the soil on the wall, Coulomb investigated the minimum force P_p which gave the most dangerous plane rupture surface. Therefore Coulomb used an extreme method of calculating and achieved his results by considering the equilibrium of the soil wedge which is failing.

This theory, although it gives admissible results when there is no wall friction, is not able to treat the earth pressure problem satisfactorily with wall friction. In the case of a wall friction the forces do not meet at a common point and static equilibrium is not satisfied as shown in figure 2. Apart from this, Coulomb's assumptions of ideal soil and plane failure surfaces are diversions from reality (13).

However, in spite of these reservations, following Coulomb, we can write the passive earth pressure formula for a vertical wall with horizontal backfill as :

$$P_p = \tfrac{1}{2}\,\gamma\,H^2\,K_p \tag{2.3}$$

where, for $\delta=0$

$$K_p = \tan^2(45 + \tfrac{\phi'}{2}) \tag{2.4}$$

The values obtained for K_p using an extension of Coulomb's theory are given in figure 3 for various values of ϕ and δ (19).

Graphical methods for determining the critical failure surface and the force at the wall were given by authors such as Poncelet and Culmann. Tables to facilitate earth pressure calculations based on Coulomb's method were prepared by Jumikis in 1962 (10).

After Coulomb, the major contribution made to the theory of earth pressures was by Rankine in 1846. Rankine in his work used the common assumptions of Coulomb, but considered a point in the soil mass and determined the forces acting at this point, A. The situation is shown in figure 4.

The point at rest is in an elastic state and by horizontal compression it changes into a plastic state which

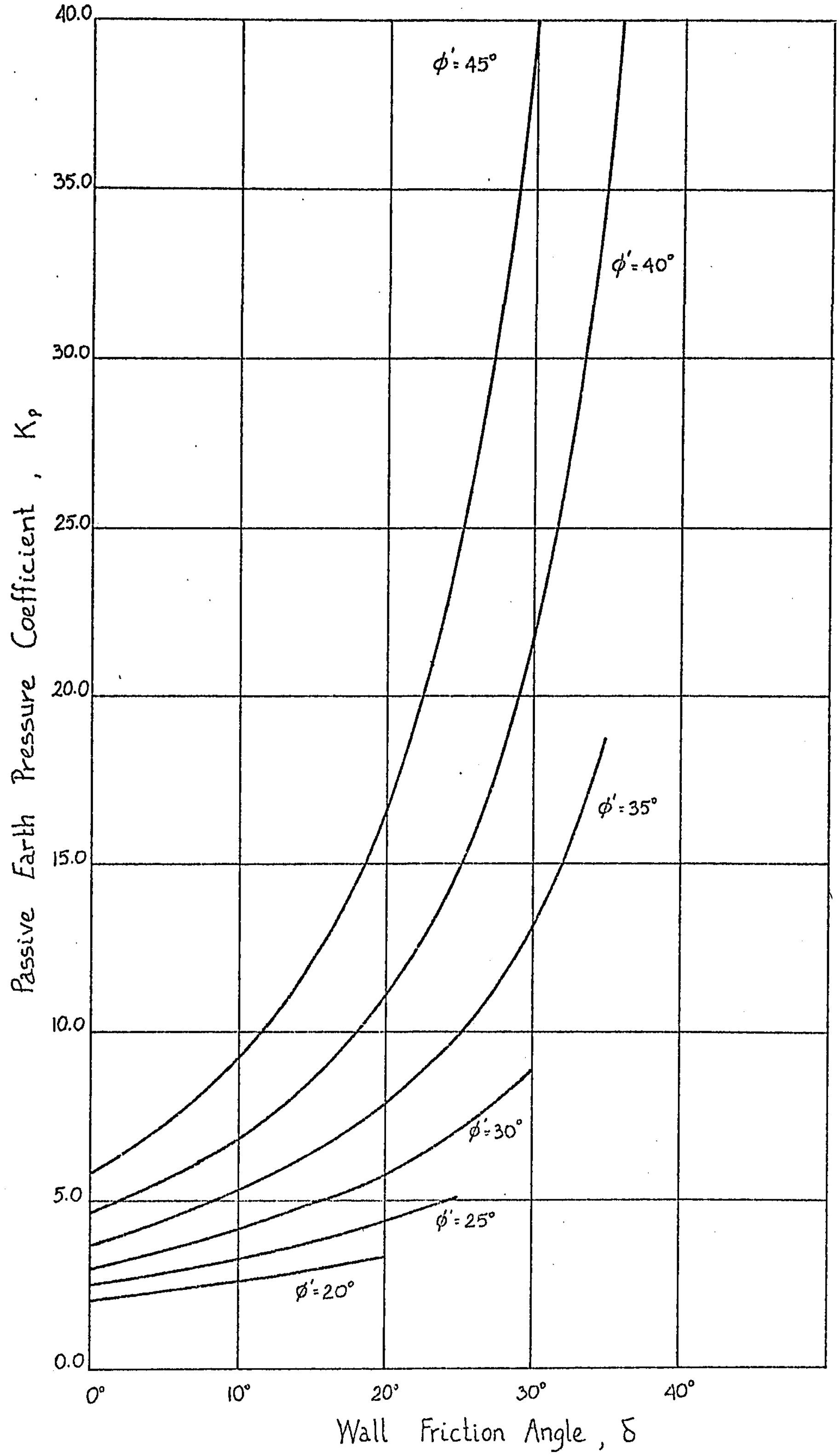

Figure 3. K_p values for dry, cohesionless sand with a horizontal surface acting against a vertical, rough wall - Coulomb's theory.

results in a passive Rankine state. The compression produces shear stresses which are equal to the strength of the soil on the paths shown in figure 4. The stress paths make angles of $(45 - \frac{\phi'}{2})$ degrees with the horizontal (see chapter 5). Having no shearing stresses on the horizontal plane, the weight of the soil, γh, above point A is the minor principal stress and the major principal stress is perpendicular to it being σ_h (13).

The situation is shown in figure 5, and with the help of a Mohr diagram we can solve for the passive earth pressure p_p. The coefficient of passive earth pressure, K_p, is defined as σ_h/σ_v and we have :

$$\sin\phi' = \tfrac{1}{2}(\sigma_h-\sigma_v)/\tfrac{1}{2}(\sigma_h+\sigma_v)$$

$$= (\sigma_h-\sigma_v)/(\sigma_h+\sigma_v)$$

$$= \{(\sigma_h/\sigma_v)-1\}/\{(\sigma_h/\sigma_v)+1\}$$

$$= (K_p-1)/(K_p+1)$$

therefore,

$$(K_p+1)\sin\phi' = K_p-1$$

then,

$$K_p = (1+\sin\phi')/(1-\sin\phi') = \tan^2(45^{\circ}+ \tfrac{\phi'}{2})$$

which is the same as Coulomb's answer for the case of a

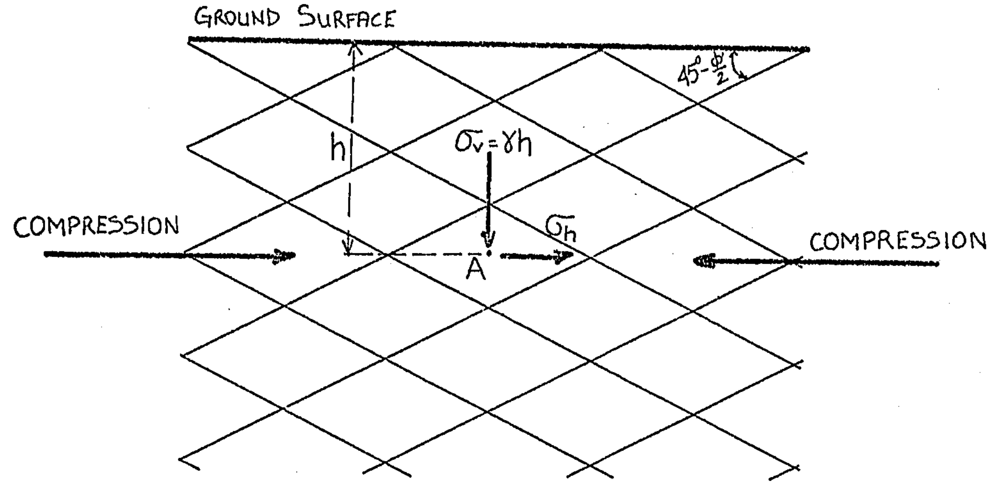

Figure 4. Stresses at a point in a semi-infinite mass of cohesionless soil, Rankine's analysis.

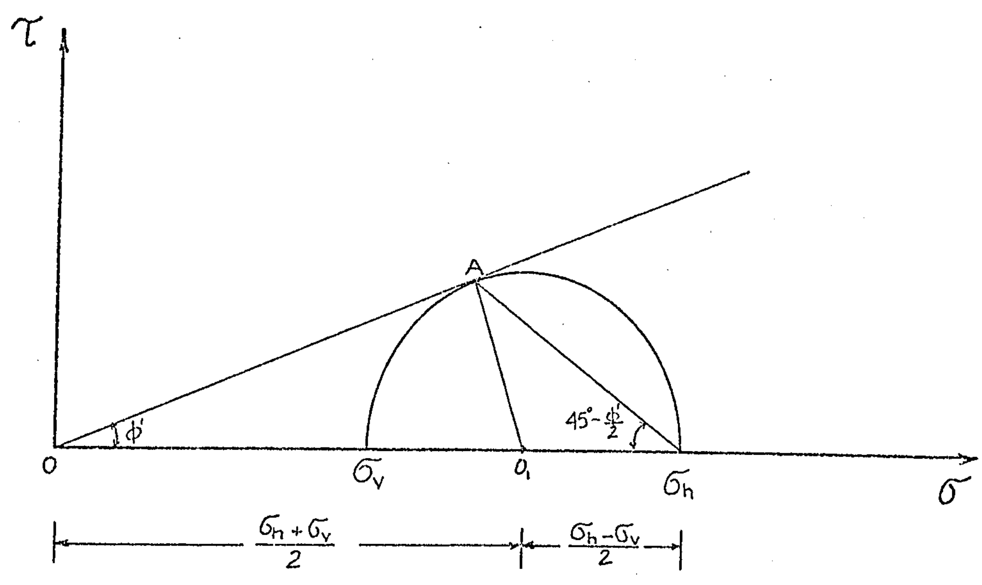

Figure 5. Mohr diagram for Rankine's analysis.

smooth, frictionless wall.

Rankine's analysis does not consider the presence of a wall and therefore it can not be used when there is wall friction. However, failure according to Rankine takes place on planes at a predetermined angle to the directions of the principal stresses. The most important effect of wall friction is that it will change the direction of the principal planes, and therefore the direction of the failure planes. Subsequent investigators have either assumed the evolution of the failure planes in the soil or have attempted to predict their generation.

Coulomb's and Rankine's methods were combined by Krey in 1936. In his 'friction circle' method Krey assumes a failure surface composed of a circular arc and a straight line (figure 6). The wedge of soil bounded by the straight line is assumed to be in a Rankine state. The resultant force R acting on the circular part of the failure surface is drawn tangent to the circle with the same center as the failure surface and radius equal to ($r' \sin\phi'$). Investigation of a failure surface which will give the minimum value of earth resistance follows the extreme method used by Coulomb. A detailed explanation of the method is given in Terzaghi's " Theoretical Soil Mechanics " (24).

K_p values obtained, using this method, are plotted in figure 7 (12).

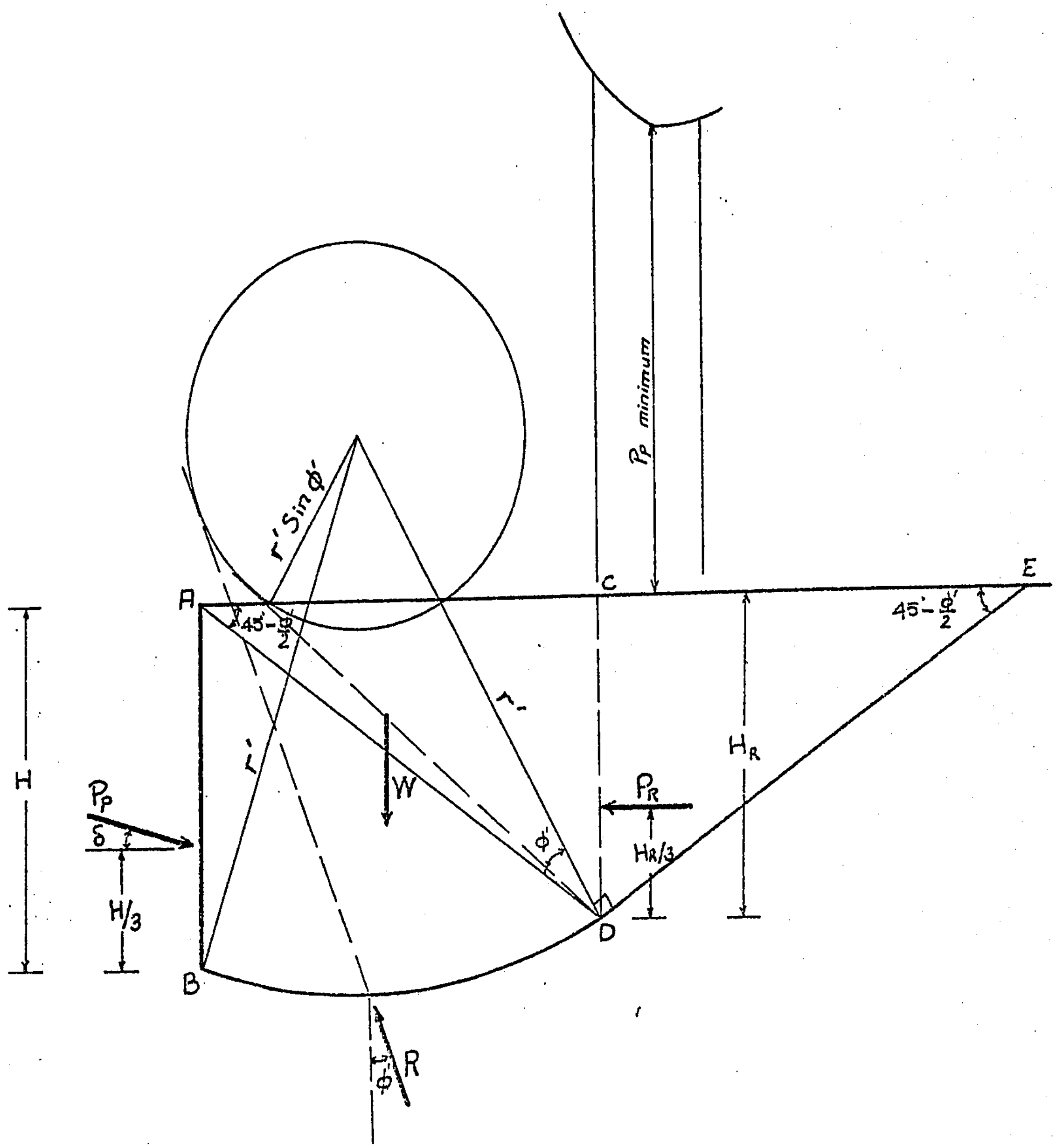

Figure 6. Passive earth pressure determination by the friction circle method for a cohesionless soil.

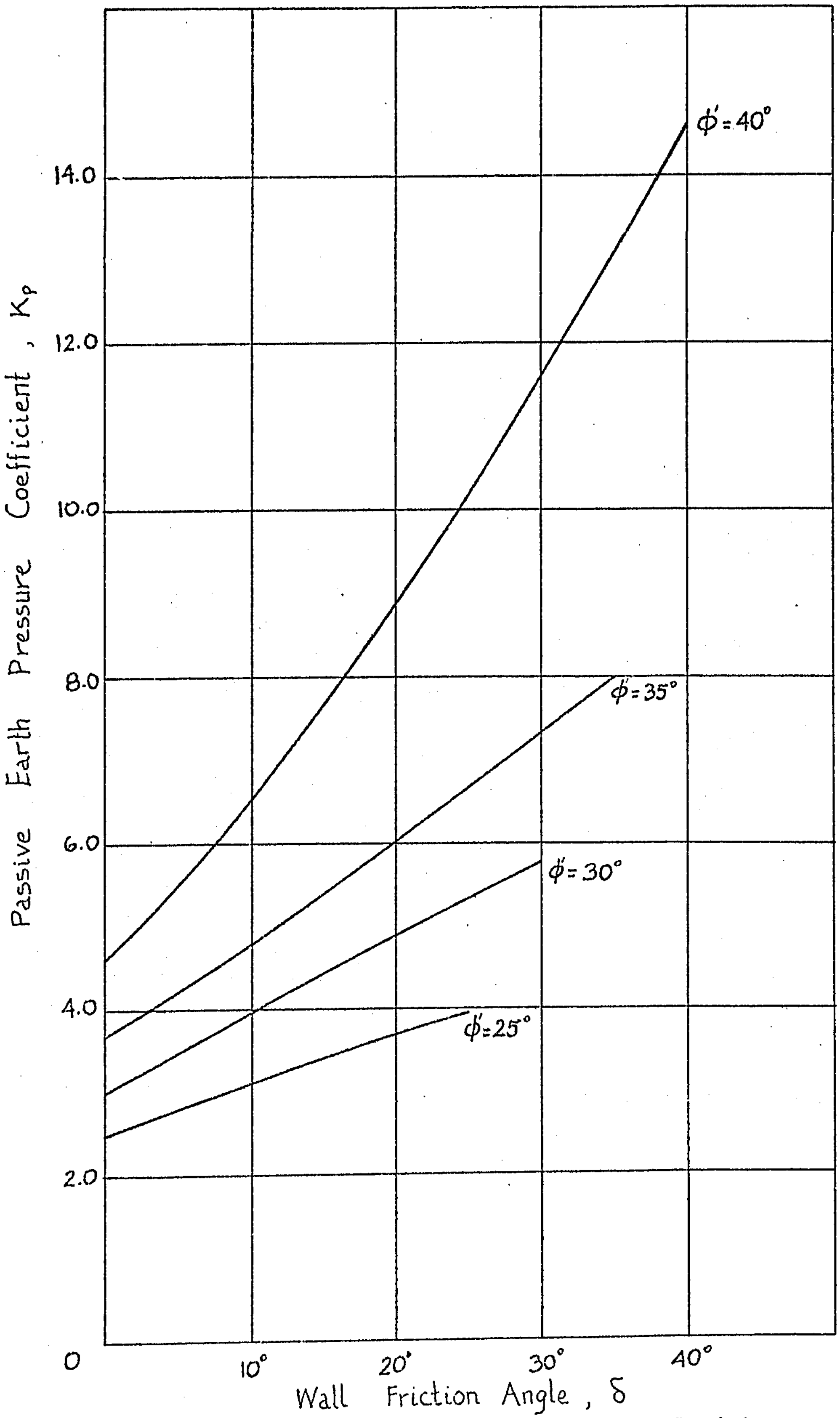

Figure 7. K_p values for dry, cohesionless sand with a horizontal surface acting against a vertical, rough wall - Friction circle method.

The circular arc failure surface of Krey was later changed into a logarithmic spiral by Ohde. Although a logarithmic spiral failure surface is thought to represent more accurately the actual failure surface, K_p values obtained for these two different surfaces do not vary largely and it is easier to deal with a circular arc than a logarithmic spiral (12).

Ohde also attempted in 1938 to combine Kötter's equation (Appendix A) with general assumptions regarding the earth pressure problem (13). If the soil is not failing as assumed, then the calculations will not be correct (24).

It will be useful at this stage to see the differance between Rankine's state of stress and Kötter's equation.

Rankine as early as 1856 had treated the state of stress of a point in the soil mass and had assumed families of parallel straight lines as surfaces of slip. Using the conditions of equilibrium in two dimensions,

$$\begin{aligned}(\partial\sigma_x/\partial x)+(\partial\tau_{xy}/\partial y) &= 0\\(\partial\sigma_y/\partial y)+(\partial\tau_{xy}/\partial x) &= \gamma\end{aligned}\qquad(2.5)$$

(see Appendix A) and substituting the values of σ_x, σ_y, τ_{xy} he solved for the resultant of passive pressures.

On the other hand Kötter in 1903 was able to write the differential equations of stresses on the rupture line, which is very useful when the general shape of the rupture line is known. By combining this equation with a boundary condition at one end, the stress on the rupture line can be determined. An earth pressure calculation can then be carried out by means of the three equilibrium conditions for the earth mass above the rupture line (5). Derivation of Kötter's equation is given in Appendix A.

In 1948 Caquot and Kerisel published passive earth pressure tables based on a theory which Caquot had worked out previously. In his theory Caquot defines an elliptic failure line with its center at the top of the wall retaining the mass. Considering a triangular slice with its vertex at the center of the ellipse and writing the equilibrium equations Caquot was able to derive the differential equations defining the state of the mass (18,27). His solution of these equations constitute the tables mentioned above and a graphical representation is given in figure 8 (2).

Assuming a logarithmic spiral failure surface, calculations of passive earth pressures were made by Terzaghi. This method is described in detail in Appendix B and the values obtained for K_p for the cases where $\phi'=\delta=30^o$ and $\phi'=\delta=40^o$ are given at the end of this chapter for comparison purposes.

Coulomb's assumptions and Kötter's equation were used in Brinch Hansen's work in 1952 (5). His work based on laboratory tests made him define the failure surface with a straight line and two circles. From this Hansen developed an empirical formula for the passive earth pressure coefficient

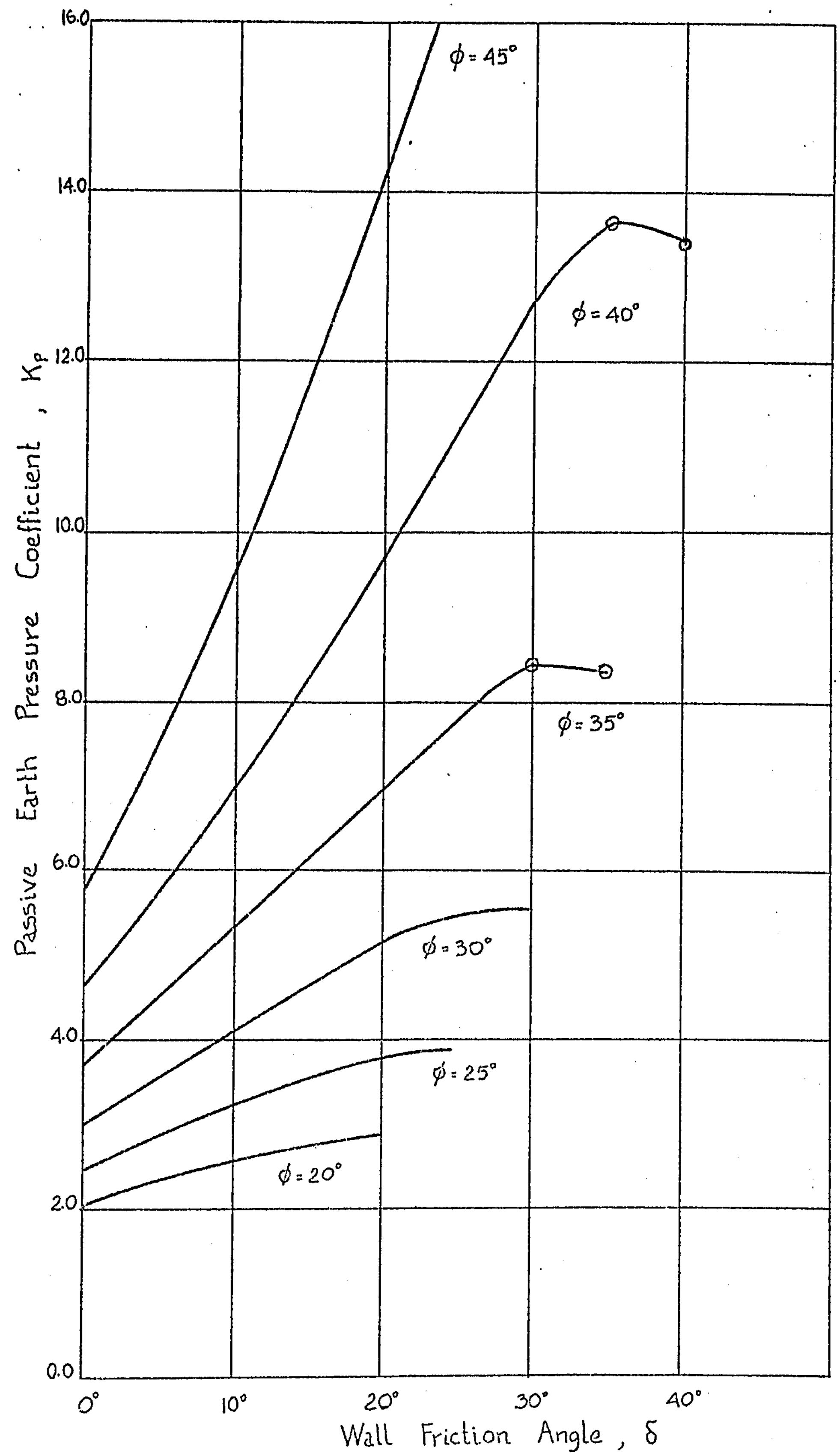

Figure 8. K_p values for dry, cohesionless sand with a horizontal surface acting against a vertical, rough wall - Caquot and Kérisel.

K_p for a rough wall. This formula is expressed as :

$$K_p = e^{\tan\phi'(\frac{1}{2}\pi+\phi')}.\cos\phi'.\tan(45^o+\frac{\phi'}{2})+0.007(e^{9\sin\phi'}-1) \tag{2.6}$$

The values obtained for K_p using equation (2.6) are given in a graphical form in figure 9.

Hansen's, Ohde's and Kötter's works formed the basis for Sokolovski's treatment of the passive earth pressure problem. In his " Statics of Soil Media " Sokolovski used the theories of plasticity. His method of solution for plane problems is developed from two basic assumptions namely: the sand is everywhere in equilibrium (equation 2.5), and the sand is everywhere yielding according to the Mohr-Coulomb criterion, given by

$$(\sigma_x-\sigma_y)^2+4\tau_{xy}^2 = (\sigma_x+\sigma_y)^2\sin^2\phi \tag{2.7}$$

If sufficient boundary conditions are known, equations (2.5) and (2.7) may be combined and solved for any region of the sand mass (6,17).

In 1957 Janbu used a generalized procedure of slices and considered the forces acting on an element of soil in the rupture zone (8). This work was similar to Bishop's slope stability analysis in 1955 (1). With this analysis Janbu could treat any shape of failure surface and he chose one which is composed of a logarithmic spiral and a straight

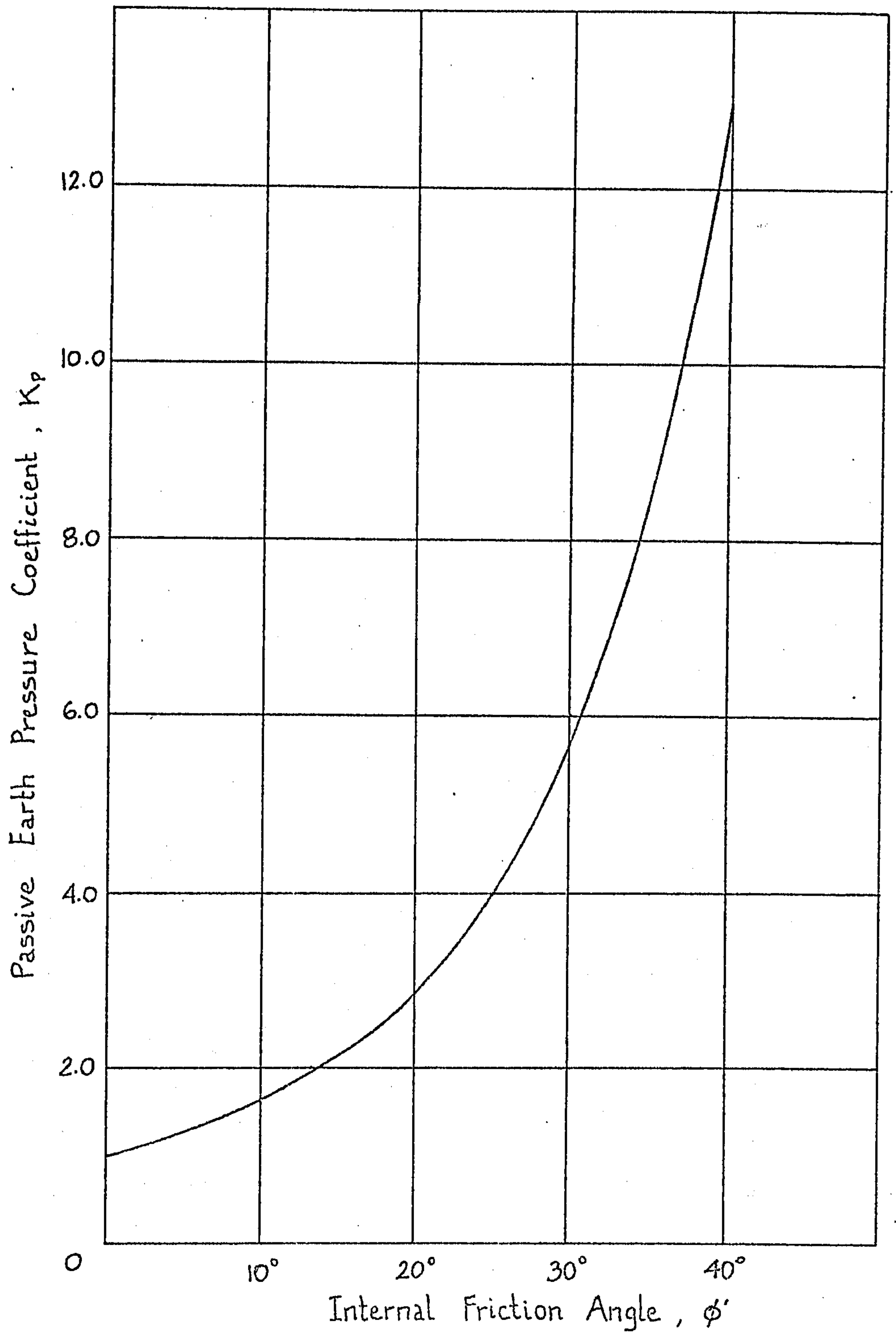

Figure 9. K_p values for a rough wall ($\phi'=\delta$), using Brinch Hansen's empirical equation.

line, in order to prepare his chart for the passive earth pressure coefficient K_p. His failure line is shown in figure 10 and a detailed explanation of his method is given in chapter 4.

In 1962 Rowe, considering only particle movement and volume change in the deformation of a soil element, ie. stress-dilatancy, was able to treat the earth pressure problem from a different, non Mohr-Coulomb point of view. However, it is Rowe's theory of the same era (14), using Mohr-Coulomb criterion and the method of slices that is considered in detail in this thesis, starting with chapter 5.

In recent years, investigators studying the passive earth pressure problem stressed the fact that the angle of internal friction for the sand, ϕ', and the wall friction angle, δ, are not constant and independent of strain. Experiments of James and Bransby (6), for example, showed this as well as the large density changes which occur in fully developed failure zones.

A simple velocity field was developed by James and Bransby in 1971 in order to explain the passive earth pressure problem (7). Their analysis studies the displacement of a rough plane wall into a mass of dry sand. Three modes of wall movements are considered : rotation about the base, rotation about the top and translation. James and Bransby attempt to idealize the material and derive the velocity field equations for the three modes of wall displacements.

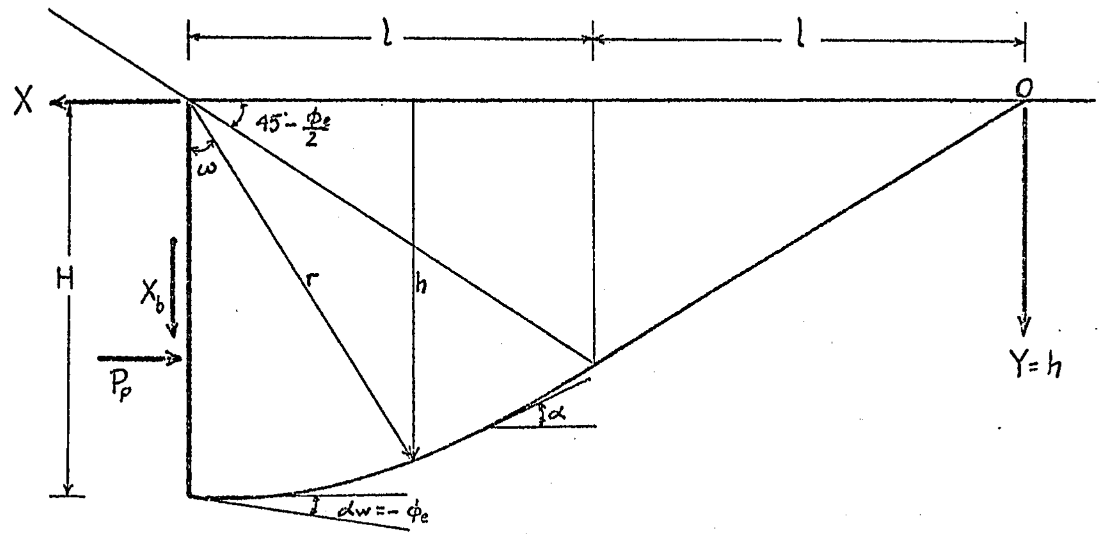

$$\phi_e = \delta$$

$$\alpha = \omega - \phi_e$$

$$\frac{L}{H} = \sin\left(45° + \frac{\phi_e}{2}\right) \cdot e^{\left(45° + \frac{\phi_e}{2}\right) \tan \phi_e}$$

$$r = H e^{\omega \tan \phi_e}$$

Figure 10. Failure surface for the passive earth pressure case for dry, cohesionless sand behind a rough vertical wall - Janbu's analysis.

The strain fields associated with these derived velocity fields are also given since they are very important in predicting the rupture surfaces. The importance of the strain is that the rupture surfaces will form only along regions of high strain. These theoretical predictions were compared with the experimental evidence obtained in 1970 by the same authors.

Later in 1971 Graham (3,4) looked for a new solution of the passive earth pressure problem. This came with the realization that assuming a constant ϕ' and δ together with the assumption of a failure occurring along a line surface seperating two rigid bodies was not in agreement with the observations. In his analysis Graham uses the numerical plasticity analysis of soils as presented by Sokolovski and calculates the passive pressures that are mobilized in cohesionless sands by self weight forces alone.

The results obtained for certain cases, using different theories are given in figure 11. From these results it is seen that when there is no wall friction all the theories give the same result and with wall friction the answers differ only slightly, with the exception of the Coulomb values. Each of these theories had to assume a failure surface. While it is obvious that a change from a wedge type of failure (Coulomb) to more free-form failure surfaces results in a dramatic change in K_p for rough walls, there is no such corresponding change in this coefficient

THEORY	PROPERTIES OF FAILURE SURFACE OR METHOD	VALUES OF K_p			
		$\phi'=30^{\circ}$		$\phi'=40^{\circ}$	
		$\delta=0^{\circ}$	$\delta=\phi'$	$\delta=0^{\circ}$	$\delta=\phi'$
Coulomb	Wedge	3.0	8.8	4.6	70.5
Rankine	State of stress in soil mass	3.0	-	4.6	-
Krey	Friction circle	3.0	5.7	4.6	14.6
Ohde	Log-spiral	3.0	5.7	4.6	14.5
Caquot	Elliptic	3.0	5.6	4.6	13.4
Hansen	Curved	3.0	5.7	4.6	14.0
Janbu	Log-spiral use of slices	3.0	6.2	4.7	14.9
Rowe	Stress-dilatancy	3.0	6.2	4.6	13.9
Terzaghi	Log-spiral	3.0	5.7	4.6	14.0
Sokolovski		3.0	5.7	4.6	14.0

Figure 11. Comparison of K_p values obtained by different theories.

among the non-wedge theories. It does not seem to matter whether the failure surface is assumed to be circular, circles and straight lines, logarithmic spiral or elliptical; whether Kotter's equation, slices, or stress-dilatancy is used also appears to have little influence on the results.

CHAPTER 3. EXPERIMENTAL REVIEW

Various experimental results are available for the case of a rotational movement or translation of a rigid wall against a granular mass. From these the value of the coefficient of passive earth pressure, K_p, may be deduced. The more important of these experiments and their results are outlined below.

The first properly executed experiments were conducted by Terzaghi in 1920 (23). With a sand height of 5 centimeters (approximately 2 inches) behind the wall, Terzaghi was able to measure the horizontal and vertical components of the earth pressure. These experiments showed a great difference in values of K_p for the loose and dense states of the soil. According to Terzaghi the passive resistance depended on two properties, the elastic properties of the material and the structure of the sand. Also the 'slip' if it occurred was of secondary importance and the earth pressure at first slip represented neither a maximum nor a minimum but something in between. The test curves for passive pressure of four materials are shown in figure 12.

Terzaghi's experiments were criticized because of the depth of sand at the wall face, which was only 2 inches. Later on in 1928 and 1929 Terzaghi used a large model to study the earth pressure problem. This setup consisted of a

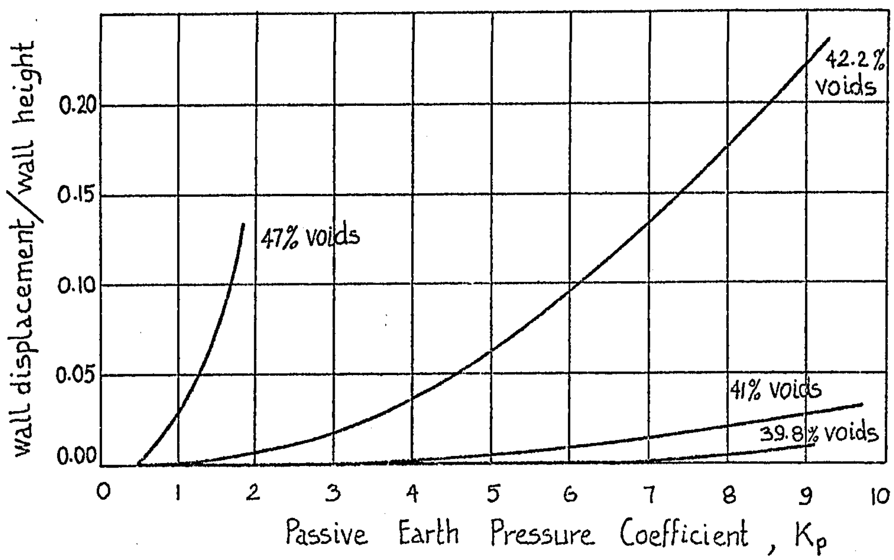

Figure 12. K_p values for sand obtained experimentally by Terzaghi in 1920.

14×14×7 feet bin and Terzaghi's main interest was to investigate the distribution of the lateral earth pressures with depth. These crude experiments proved that the distribution of pressures against a retaining structure is a function of the nature of the wall displacements (26).

In 1924 and 1928 Franzius used a rigid wall with translatory movement and attempted to measure the K_p values. His experiments continued to 1934 and the model he used was a wall 2 meters by 2 meters. Franzius reported that double the Rankine coefficients could be used in designs for passive earth pressure. Doubling the Rankine values however, does not give the large differences between the loose and dense states found by Terzaghi. The side friction of the bin influenced the measurement of earth pressure and to compensate for this, Franzius reduced the measured values of K_p by 10 percent.

These test results were criticized from the point of view of the percentage of load attributed to side friction and the interpretation of the sand properties. Franzius' test results were lower than the existing theoretical values for K_p (13).

Tests by Tschebotarioff and Johnson using a large apparatus which provided a $\delta>0$ boundary condition, in 1953, showed that the Rankine values were not high enough to represent these cases. Theoretical values of Caquot and Kerisel were shown to be excessive by these experiments.

The inability to control the wall friction or the rotation of the wall during the tests was the main criticism for these experiments. The side wall friction was measured during the experiments, but was not considered in the calculation of K_p (13).

Terzaghi's results were confirmed in 1961 by Schofield. Using a sharp edged, rigid, flat, 6 inches by 6 inches square plate Schofield studied the earth pressure problem. After the experiments he concluded that calculating passive lateral resistance of soil, assuming a unique value of wall friction angle δ, is not correct because in an experiment δ varied from +0.3 radians to -0.2 radians before failure (16).

The passive earth pressure in sands was studied carefully by Peaker in 1964. The results showed that simply inserting the peak values of ϕ' and δ from independent tests into theoretical expressions did not give correct results for the passive earth pressure coefficients for rough walls. Peaker stressed the fact that consideration of the wall movement and the mobilization of ϕ' and δ seemed critical to finding a satisfactory theory and he recommended values for K_p (13,15).

In 1969 Narain, Saran and Nandakumaran used a model 59×35×24 inches and considered the translation of a wall as well as its rotation about the top and bottom edges. Their aim was to determine the rupture surfaces and record the pressures on the wall. After the tests they concluded that the magnitude of the passive pressure and its distribution over the height of the wall and the shape of the rupture wedge formed behind the wall depend on the type of displacement given to the wall. Only in the case of wall translation was the passive pressure distribution found to be triangular. In the two other cases the distribution is close to a parabola. None of the more common theories was found to give the passive earth resistance or the size and shape of the rupture wedge correctly. Part of their test results are shown in figure 13 (11).

Experiments by James and Bransby in 1970 were conducted with an initially vertical, rough, plane wall rotated about its toe into a mass of dry sand. Their results stress the difference in the values obtained for dense and loose sands in passive pressure measurements as well as the non-linearity of the normal stress distribution on the wall with depth. Rupture surfaces were also studied by the authors using an X-ray technique (6).

Tcheng and Absi in 1969 started conducting large scale earth pressure experiments (20). Tcheng's continuing work made him conclude that the passive earth pressure coefficient is actually smaller than the value given by theory (21). In fact, for a horizontal soil surface and a vertical wall, the experimental value of the coefficient was found to be half the value given by theory (22).

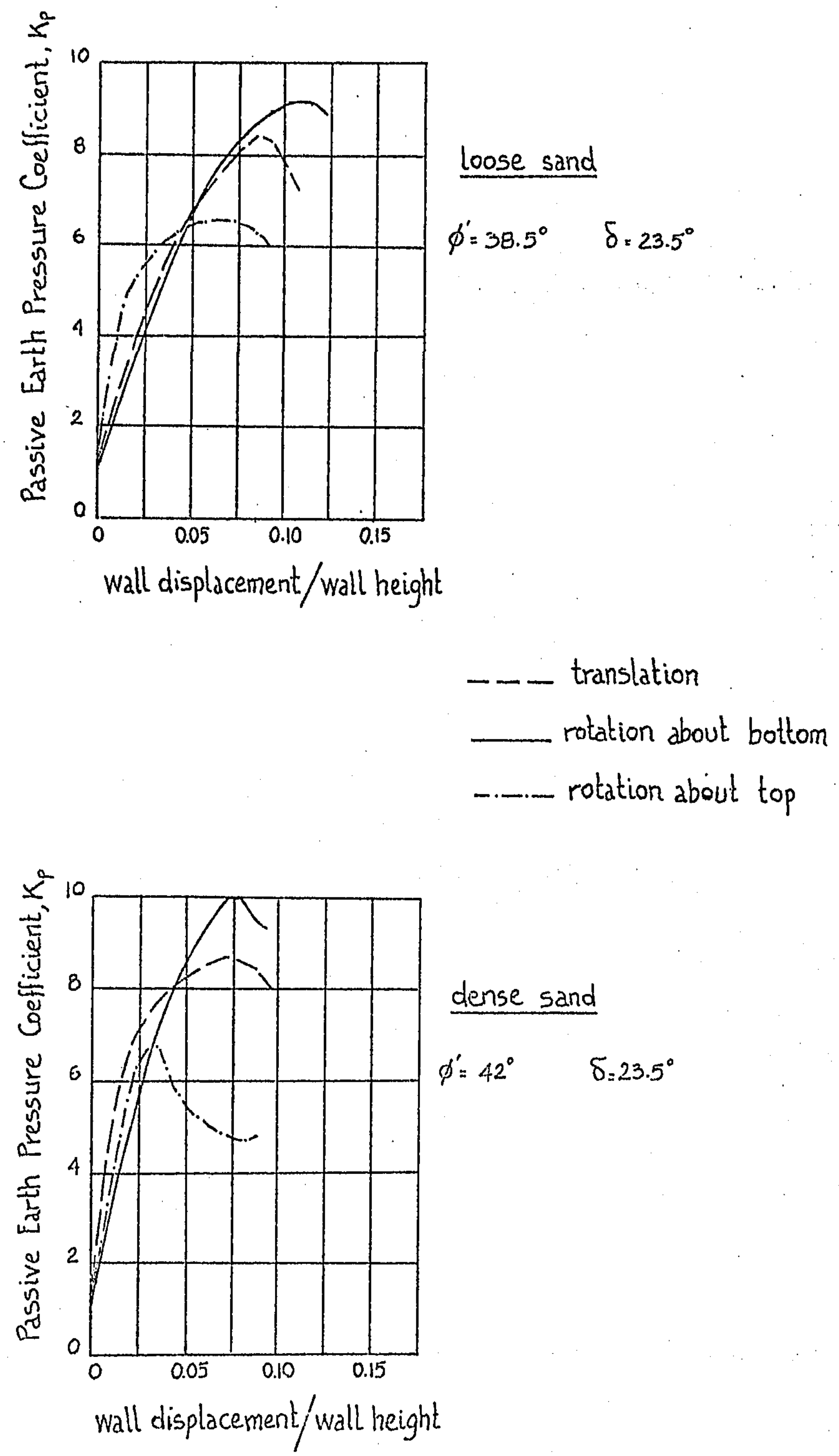

Figure 13. Experimental measurements of K_p as a function of wall displacement by Narain et al.

PART II. THEORETICAL ANALYSIS

CHAPTER 4. JANBU'S ANALYSIS

CHAPTER 5. ROWE-COULOMB METHOD

CHAPTER 4. JANBU'S ANALYSIS

The stability analyses commonly used presently are determinate analyses; that is, the equations of equilibrium are combined with a failure criterion to obtain a bound solution. The strain state is not considered directly. The slightest movement is sufficient to develop the failure along the proposed slip surface, showing the soil as effectively rigid-plastic. In these analyses (for example Coulomb and Rankine) the failure surfaces must be assumed and certain boundary conditions must be stated.

In order to overcome the difficulties arising from the application of the classical plasticity theory to heterogenous soil masses the method of slices was found to be suitable as used by Bishop in his slope stability analysis and Janbu in his earth pressures analysis (1,8). The statical equations of a slice can be written in a general form for determining the earth pressures.

Consider the forces acting on the system and on the slice in figures 14 and 15 respectively. The shearing resistance τ_f along an element of potential slip surface is given in terms of the effective normal stress, σ', by :

$$\tau_f = c'+\sigma'\tan\phi' \qquad (4.1)$$

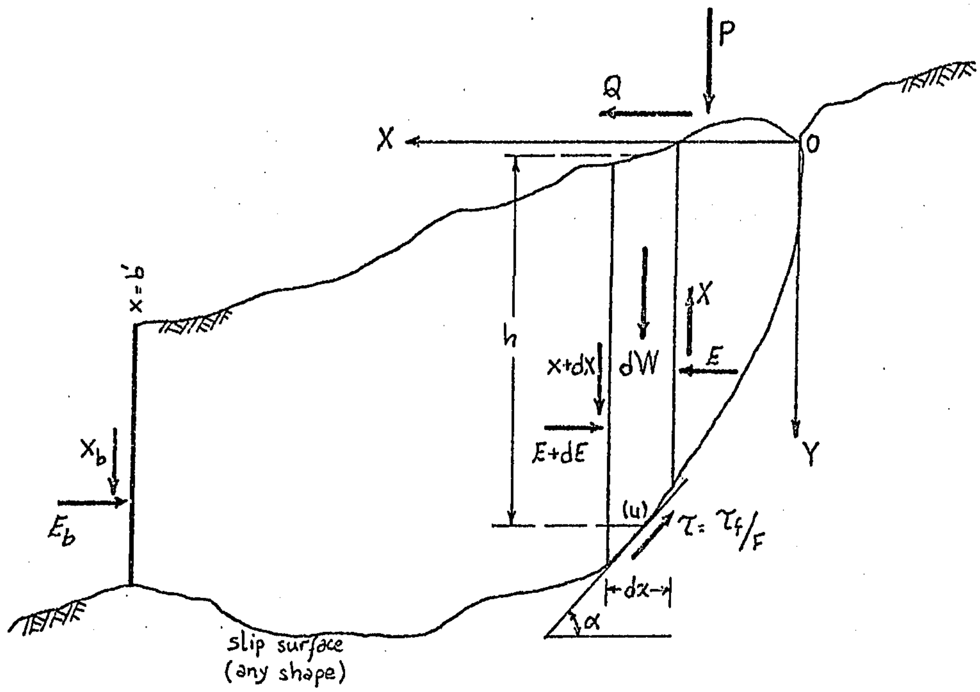

Figure 14. Forces acting on a general passive earth resistance system - Janbu's analysis.

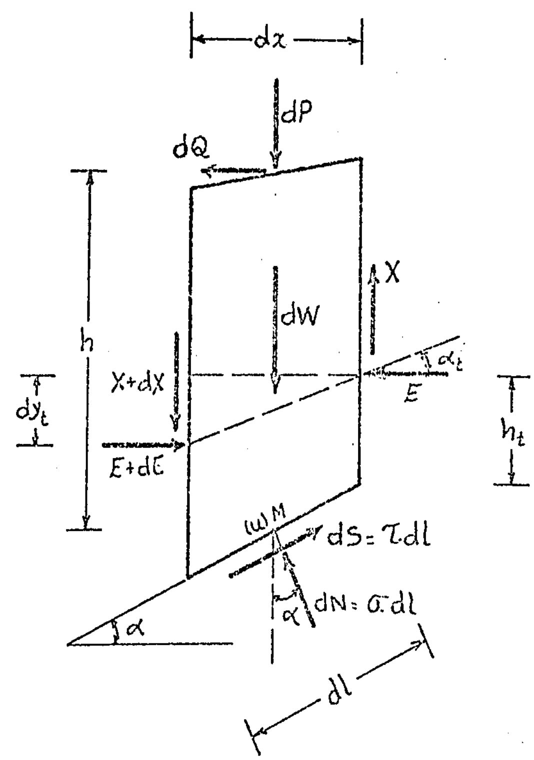

Figure 15. Forces acting on a slice element Janbu's analysis.

Along this element the shearing stress τ, necessary to maintain equilibrium can be expressed as a certain portion of τ_f :

$$\tau = \frac{\tau_f}{F} = c_e + \sigma' \tan\phi_e \tag{4.2}$$

Considering the equilibrium for each slice :

Σvertical forces=0

$$dW+dP+dX = dS\sin\alpha + dN\cos\alpha \tag{4.3}$$

Σhorizontal forces=0

$$dE-dQ = -dS\cos\alpha + dN\sin\alpha \tag{4.4}$$

Σmoments about point M=0

$$Xdx+Edy_t - dE.h_t + dQ.h = 0 \tag{4.5}$$

also,

$$\int_o^{b'} dX = X_b \quad \text{and} \quad \int_o^{b'} dE = E_b \tag{4.6}$$

Let $$p = \frac{dW}{dx} + \frac{dP}{dx} \quad \text{and} \quad t = \frac{dX}{dx} \tag{4.7}$$

From equation (4.3) and noticing that, $\sigma' = \frac{dN}{dl} - u$

$$\sigma' = (p+t-u) - \tau\tan\alpha \tag{4.8}$$

using equations (4.2) and (4.8) we will obtain :

$$\tau = \frac{c_e + (p+t-u)\tan\phi_e}{1+\tan\alpha.\tan\phi_e} \qquad (4.9)$$

On the other hand, eliminating dN from equations (4.3) and (4.4) :

$$dE = dQ + (p+t)\tan\alpha.dx - \tau\cos^{-2}\alpha.dx \qquad (4.10)$$

With this equation the horizontal force E at any vertical section is obtained by integration between the limits zero and x. The corresponding shear force X can be found in terms of E and Q, if equation (4.5) is divided by dx :

$$X = -E\tan\alpha_t + h_t.\frac{dE}{dx} - h.\frac{dQ}{dx} \qquad (4.11)$$

From equations (4.6) and (4.10) the following expression for the normal force at the wall can be written :

$$E_b = Q + \int_0^{b'} (p+t)\tan\alpha.dx - \int_0^{b'} \tau\cos^{-2}\alpha.dx \qquad (4.12)$$

Since in the above derivation no simplifying assumption has been made regarding the shape of the potential slip surface, the criterion is applicable to any chosen slip surface.

The stability criterion can be written considering a specified value of F, by substituting the expression for τ from equation (4.9) into equation (4.12) and noting that $\tan\alpha . dx = dy$. Then :

$$E_b - \int_0^{b'} u.dy = Q + \int_0^{b'} \{(p+t-u) + c_e \cot\phi_e\} \tan(\alpha - \phi_e) dx - \int_0^{b'} c_e \cot\phi_e . dy \qquad (4.13)$$

If $\tau_f = F\tau$ is introduced into equations (4.9) and (4.12) for determining F, the following working formula can be obtained for finite differences :

$$F = \frac{\Sigma \tau_f \cos^2\alpha . \Delta x}{Q - E_b + \Sigma (p+t) \tan\alpha . \Delta x} \qquad (4.14)$$

where,

$$\tau_f = \frac{c' + (p+t-u) \tan\phi'}{1 + \tan\alpha . \tan\phi' / F}$$

The quantity t contained in the working formulae is statically indeterminate when the actual stress conditions are not known. By assuming the line of thrust, accurate values of the corresponding internal forces E and X can be obtained from equations (4.10) and (4.11) by successive approximations. First E_o and X_o are calculated for the condition t=0. From X_o, $t_o = dX_o/dx$ can be obtained which when introduced into equations (4.10) and (4.11) will lead to improved values E_1 and X_1, and so on.

In order to apply these equations to a passive earth pressure problem, dry sand behind a vertical wall is considered. Figure 16 shows the situation.

By introducing $c'=0$, $u=0$, $Q=0$ and $E_b=P_p$ into equation (4.13), the passive force is obtained as :

$$P_p = \int_o^{b'} (p+t)\tan(\alpha+\phi_e)\,dx \tag{4.15}$$

also,

$$X_p = P_p \tan\delta_e \tag{4.16}$$

The boundary condition in the vertical direction along b'-b' is established by introducing equations (4.16) and (4.10) into equation (4.11) :

$$\tan\delta_e = -\tan\alpha_{tw} + \frac{H_t}{P_p}(\gamma H+q+t_w)\tan(\alpha_w+\phi_e) \tag{4.17}$$

To apply equations (4.15) and (4.17) to composite failure surfaces, the line of thrust is drawn through the lower third points of each slice. For the initial investigation, conditions t=0 and q=0 are considered.

Equations (4.15) and (4.17) can be written in the following forms :

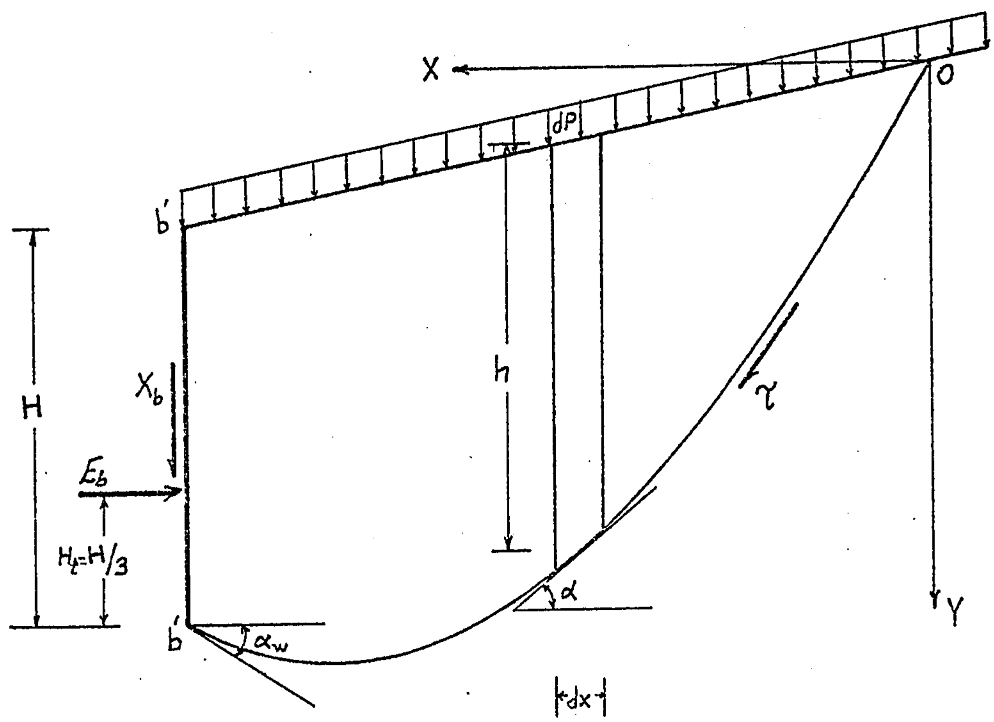

Figure 16. Passive earth pressure analysis with dry sand behind a vertical wall, Janbu's method.

$$K_p = \frac{2}{H^2} \int_o^{b'} h.\tan(\alpha+\phi_e)\,dx \tag{4.18}$$

$$\tan\delta_e = -\frac{2}{3}\tan\alpha_w + \frac{2}{3K_p}\tan(\alpha_w+\phi_e) \tag{4.19}$$

With these equations for a given value of ϕ_e corresponding values of K_p and δ_e can be obtained for any chosen slip surface.

K_p values calculated by Janbu using a logarithmic spiral and straight line composite surface are given in figure 17.

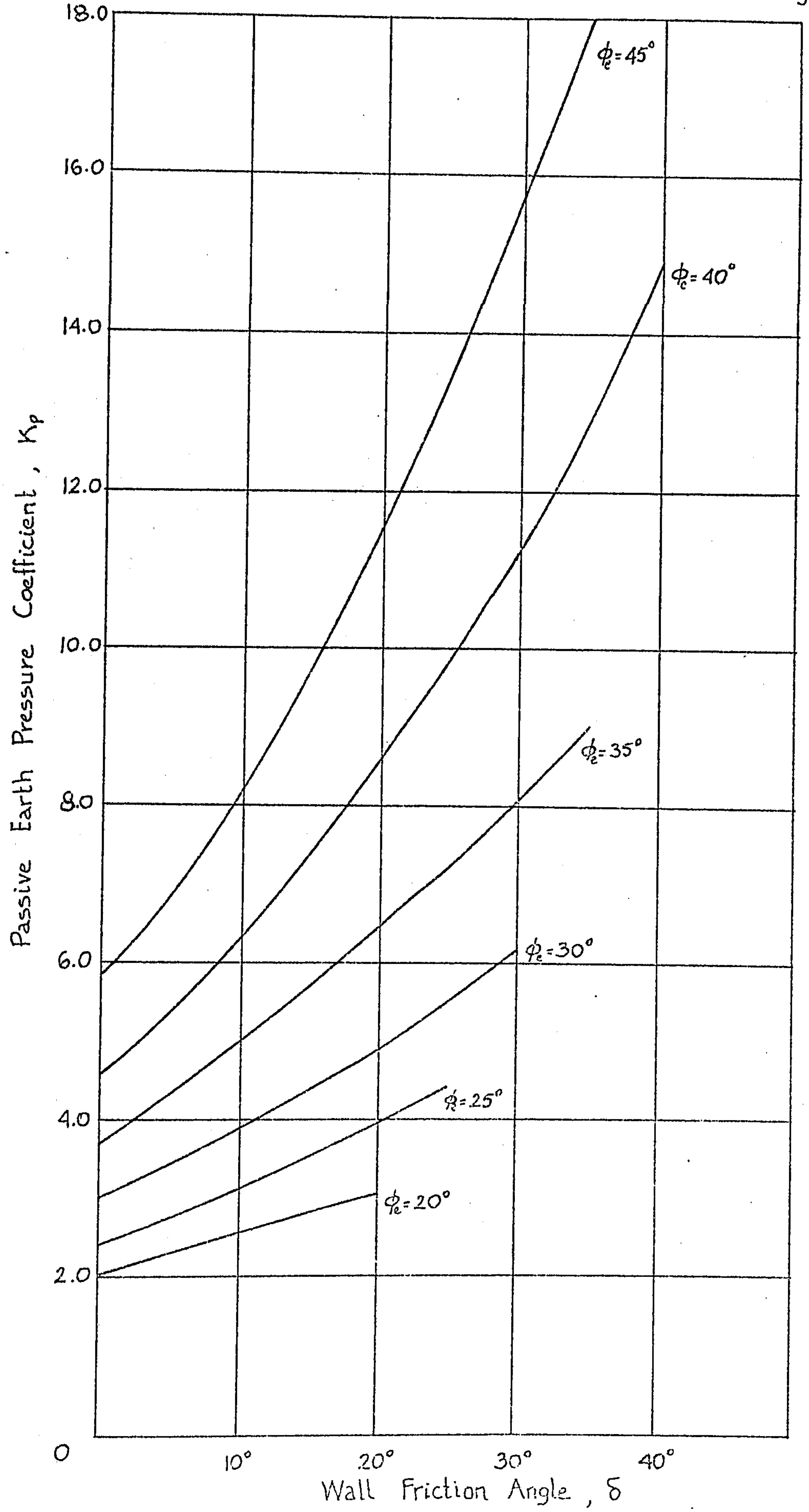

Figure 17. K_p values, Janbu's analysis.

CHAPTER 5. ROWE-COULOMB METHOD

A second analysis using the method of slices and Mohr-Coulomb strength parameters is attributable to Rowe. it will be referred to as the Rowe-Coulomb method in order to distinguish it from Rowe's stress-dilatancy work.

The Rowe-Coulomb method is used to calculate the passive earth pressure coefficients for dry, ideal sands represented by ϕ' and γ, behind a rough, vertical wall with a wall-soil friction angle of δ.

Rowe's work is not published and for that reason a detailed derivation of his equation will be given here.

Consider the forces on a slice in the passive state for a chosen α-line (slip line), and the force diagram shown in figures 18 and 19 respectively.

From the geometry of the force diagram :

$$AB+BD = AI+ID$$

therefore,

$$(W+dX)\sin(\alpha+\phi')+c'l.\cos\phi' = dE.\cos(\alpha+\phi')+ul.\sin\phi'$$

where

$$l = b/\cos\alpha$$

then,

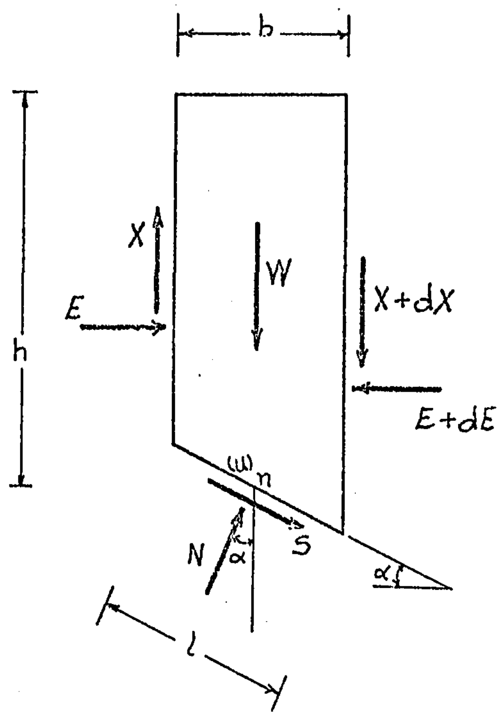

Figure 18. Forces acting on a slice in the passive state for a chosen α-line.

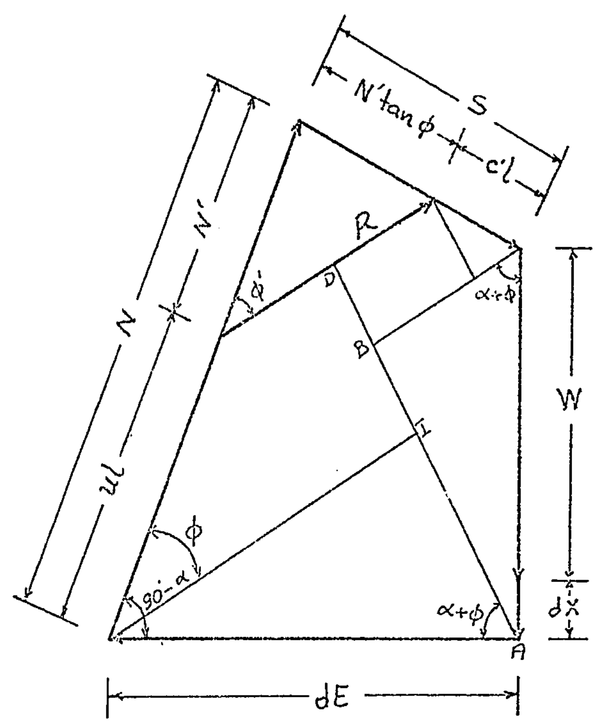

Figure 19. Force diagram for the slice.

$$(W+dX)\sin(\alpha+\phi')+c'b\frac{\cos\phi'}{\cos\alpha} = dE.\cos(\alpha+\phi')+ub\frac{\sin\phi'}{\cos\alpha}$$

$$dE.\cos(\alpha+\phi') = (W+dX)\sin(\alpha+\phi')+\frac{b}{\cos\alpha}(c'\cos\phi'-u.\sin\phi')$$

therefore,

$$dE = (W+dX)\tan(\alpha+\phi')+\frac{b}{\cos\alpha}\{\frac{c'\cos\phi'-u.\sin\phi'}{\cos(\alpha+\phi')}\} \tag{5.1}$$

For the special case of $c'=u=0$, equation (5.1) becomes :

$$dE = (W+dX)\tan(\alpha+\phi') \tag{5.2}$$

It is of interest to note the derivation of the special Rankine case with this analysis. The slip line in this cohesionless, no wall friction case is a straight line and forms a slip wedge (figure 20). If the failure wedge is considered as one slice, the following will hold :

$$E = 0$$

$$X = 0$$

$$X+dX = 0$$

Substituting these into equation (5.1), together with :

$$b = H.\tan(45^{\circ}+\tfrac{1}{2}\phi')$$

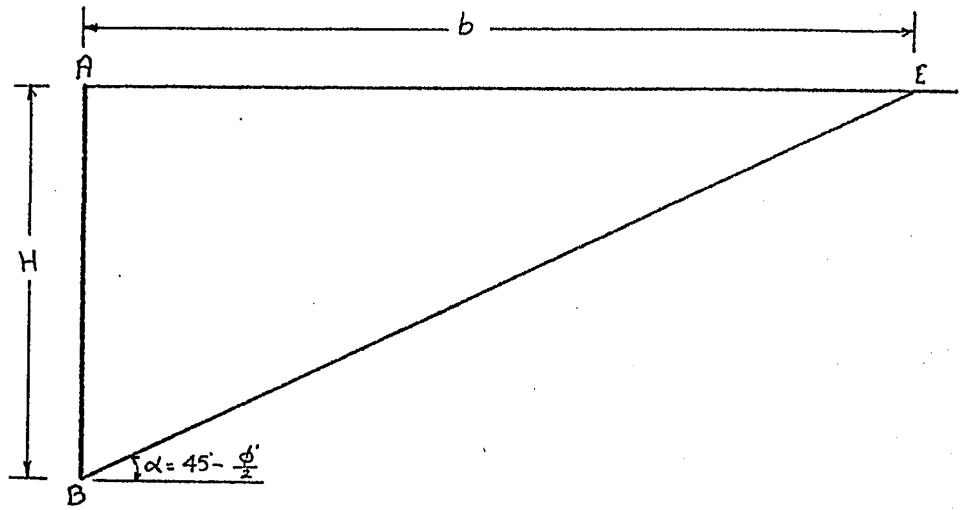

Figure 20. Failure surface for Rankine case with c'=0, u=0 and δ=0.

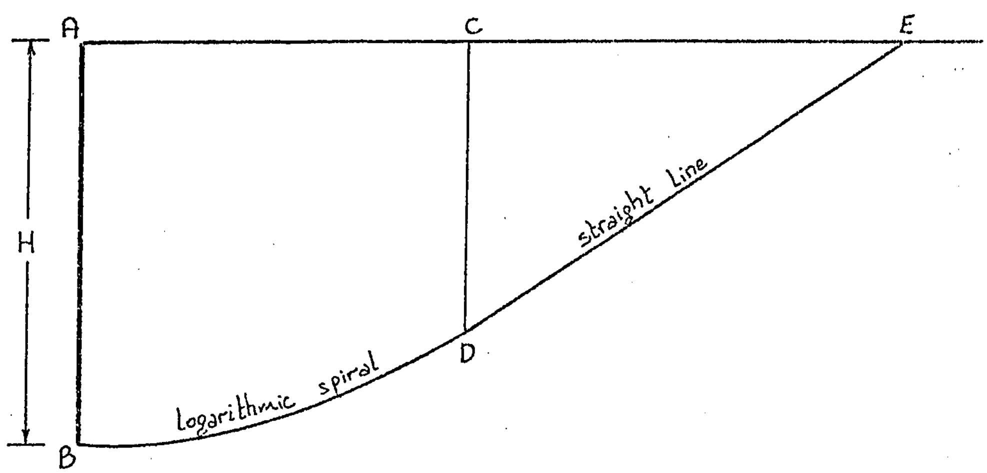

Figure 21. Rowe's failure surface.

$$W = \tfrac{1}{2}\gamma Hb = \tfrac{1}{2}\gamma H^2 \tan(45^{\circ}+\tfrac{1}{2}\phi')$$

$$dX = 0$$

$$c' = 0$$

$$u = 0$$

we obtain :

$$dE = \tfrac{1}{2}\gamma H^2 \tan^2(45^{\circ}+\tfrac{1}{2}\phi')$$

where,

$$dE = P_p \quad \text{and} \quad \tan^2(45^{\circ}+\tfrac{1}{2}\phi') = K_p$$

which is identical with the Rankine equation.

For the more general case of a rough wall, Rowe considers a failure surface made up of a logarithmic spiral and a straight line which is shown in figure 21. His reasoning appears to be that it has been shown that the use of a logarithmic spiral-straight line failure surface give results of the same order as other more complex shapes such as the ellipse, circles, etc.

The properties of the logarithmic spiral are shown in figure 22.

The radius vector, r, is given by the equation :

$$r = r_o e^{\theta \tan\phi'} \tag{5.3}$$

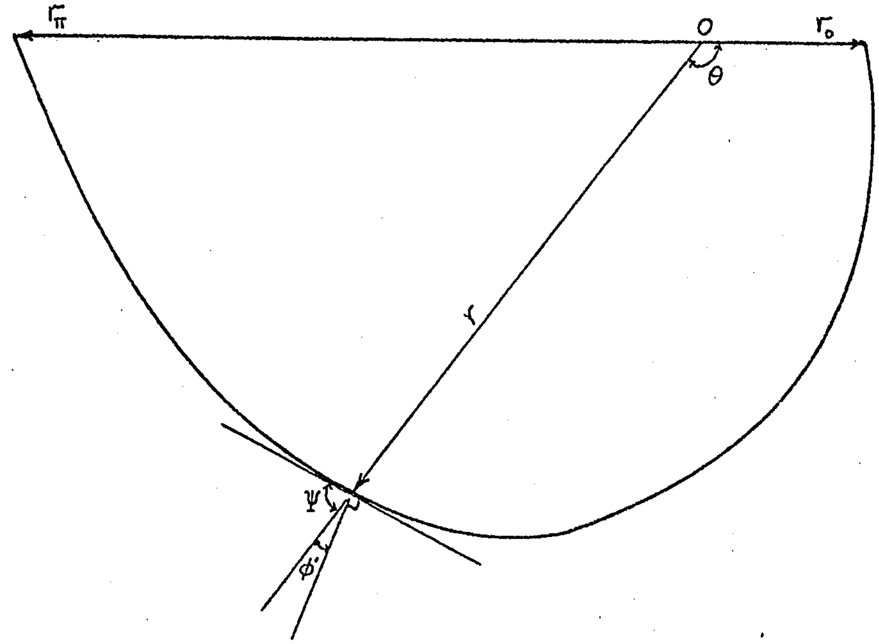

Figure 22. Properties of the logarithmic spiral.

The angle ϕ' is the angle between the radius vector and the normal to the curve where the radius vector meets the curve. The angle ϕ' is chosen so that the resultants of the normal and shear forces acting on the failure surface will pass through the common point O, the center of the logarithmic spiral, and therefore will create no unbalanced moments due to the resistance of the soil.

The angle between the tangent to the curve and the radius vector at that point is equal to Ψ which is a constant. Therefore the relation :

$$\Psi = \tfrac{1}{2}\pi - \phi' \tag{5.4}$$

holds.

Vertical shear at the wall is assumed to be present which will dissipate and disappear at some horizontal distance from the wall. Beyond this point there will be no vertical shear and by definition it will be in a Rankine state. Being in a Rankine state this portion of the failure line will be straight and will bound a wedge of soil (figure 23).

The angle $(45^{\circ} - \tfrac{1}{2}\phi')$ which the line CE makes with the horizontal can be verified by considering the stresses on an element of soil as follows.

When a two dimensional element of soil is stressed to failure under principal stresses σ_1 and σ_3, failure will occur along a slip plane inclined at an angle α with the

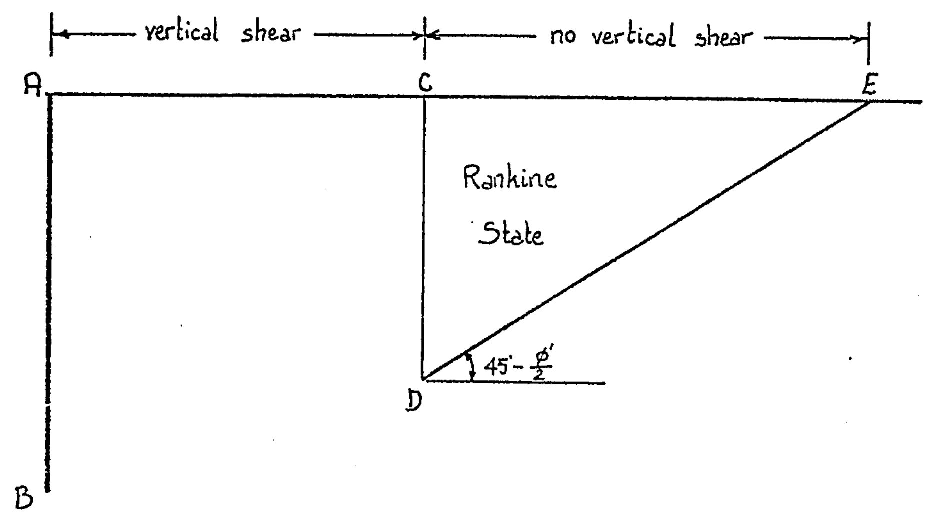

Figure 23. Development of Rowe's failure surface.

major principal plane (figure 24). The normal and shear stresses on the failure surface are given by :

$$\sigma = \tfrac{1}{2}(\sigma_1+\sigma_3)+\tfrac{1}{2}(\sigma_1-\sigma_3)\cos 2\alpha \qquad (5.5)$$

$$\tau = \tfrac{1}{2}(\sigma_1-\sigma_3)\sin 2\alpha \qquad (5.6)$$

Substituting equations (5.5) and (5.6) into the failure criterion equation,

$$\tau = c+\sigma\tan\phi' \qquad (5.7)$$

the following equation is obtained :

$$\tfrac{1}{2}(\sigma_1-\sigma_3)\sin 2\alpha = c+\tfrac{1}{2}\{(\sigma_1+\sigma_3)+(\sigma_1-\sigma_3)\cos 2\alpha\}\tan\phi' \qquad (5.8)$$

Using the trigonometric relationships :

$$\sin 2\alpha = 2\sin\alpha.\cos\alpha$$

and

$$\cos 2\alpha = 2\cos^2\alpha-1$$

equation (5.8) becomes,

$$\sigma_1\sin\alpha.\cos\alpha-\sigma_3\sin\alpha.\cos\alpha = c+\tan\phi'\{\sigma_3+(\sigma_1-\sigma_3)\cos^2\alpha\}$$

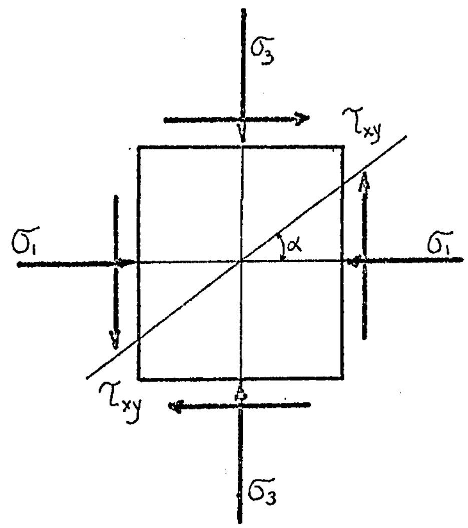

Figure 24. Stresses on a two dimensional element of soil with α failure plane.

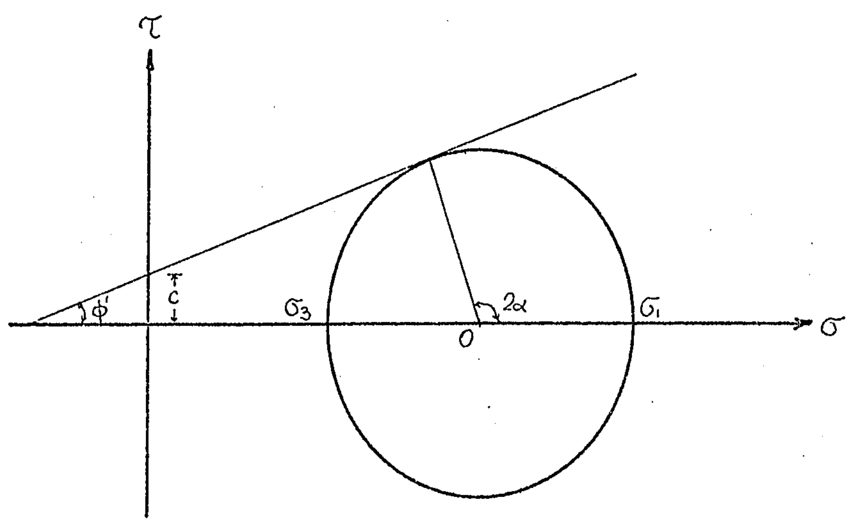

Figure 25. Mohr circle representation of the stresses on an element of soil with α failure plane.

or,

$$\sigma_1 = \sigma_3 + \frac{c+\sigma_3\tan\phi'}{\sin\alpha.\cos\alpha-\cos^2\alpha.\tan\phi'} \tag{5.9}$$

Figure 25 shows a Mohr circle representation of this condition. The quantity α is determined by the condition that the stresses on the failure plane are the critical ones and control the value of σ_1 for a given value of σ_3. The failure plane is the one with angle α that gives a minimum value of σ_1 for a given value of σ_3. Therefore,

$$\frac{d}{d\alpha}(\sin\alpha.\cos\alpha-\cos^2\alpha.\tan\phi') = 0$$

then,

$$\cos^2\alpha-\sin^2\alpha+2\tan\phi'.\sin\alpha.\cos\alpha = 0$$

therefore,

$$\alpha = 45^{\circ}-\tfrac{1}{2}\phi'$$

Since the stresses are symmetrical with respect to the 1 and 3 axes, there are two sets of failure planes making angles of $\pm\alpha$ with the major principal axis (figure 26). In the passive case the major principal stress is σ_1 and therefore the major principal axis is the 3-axis. The angle between the horizontal and the failure plane is therefore

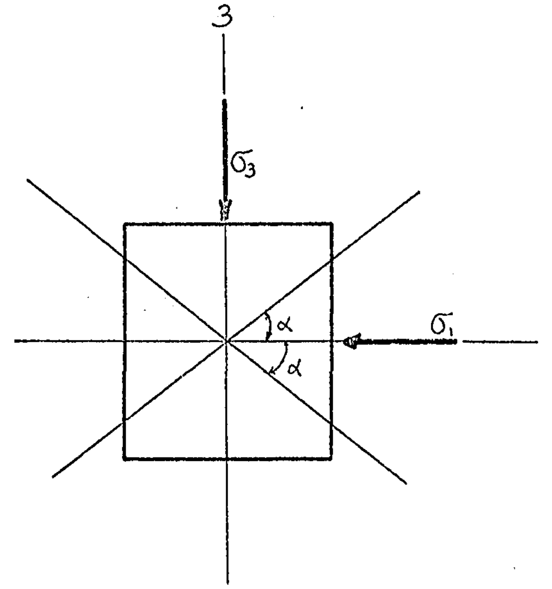

Figure 26. Failure planes on a two dimensional element of soil.

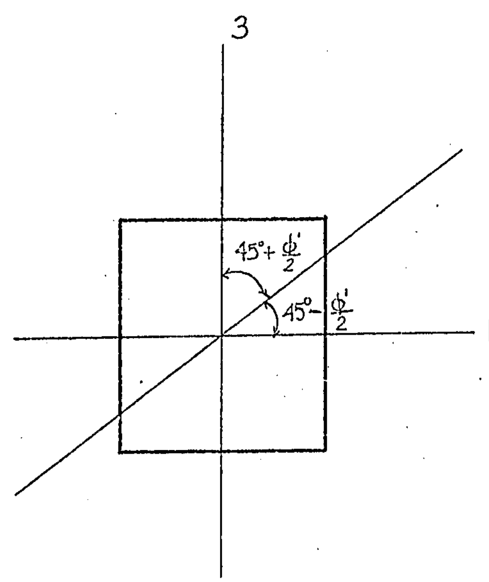

Figure 27. Inclination of the failure plane to the horizontal on a two dimensional element of soil.

equal to ($45^{\circ}-\frac{1}{2}\phi'$) as shown in figure 27 (28).

From figure 26 it is seen that there are two possible Rankine surfaces, one being the kinematically admissable failure surface. The other surface is the conjugate failure surface. In order to accommodate the Rankine zone and the conjugate failure surface the distance from the wall to the Rankine zone, AC, is a function of the height CD (figure 23) and therefore the conjugate surface must be AD.

The remaining portion, BD, of the failure surface is a logarithmic spiral. For this curved surface to join smoothly with the straight line, Rankine surface at D, the tangent to the logarithmic spiral at D must have the direction of DE. By geometry it may be shown that this condition is satisfied when the conjugate failure surface is a ray of the logarithmic spiral. From figure 28 :

$$\angle EDG = 90^{\circ}-\phi'$$

therefore,

$$\angle EDG = \Psi$$

Therefore extension of the line GD is a ray (radius vector) of the logarithmic spiral which is also the conjugate failure line.

The foregoing implies that the center of the logarithmic spiral must be located on the conjugate failure plane AD or on its extension.

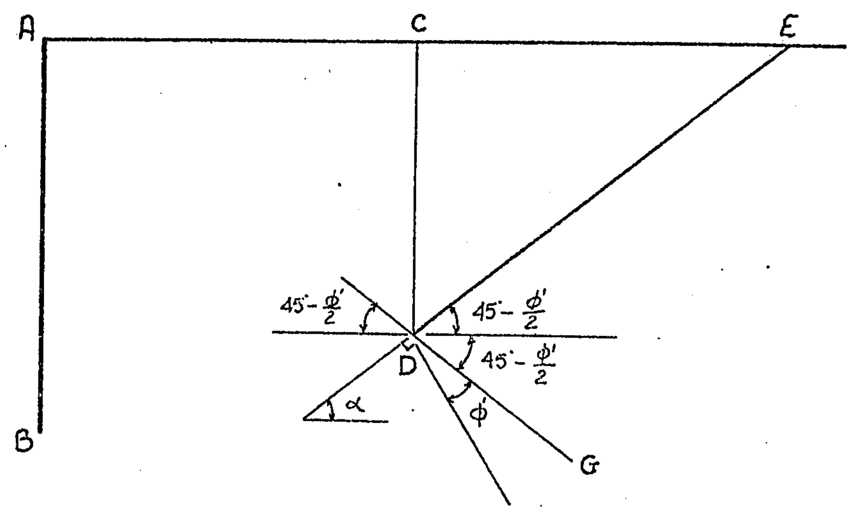

Figure 28. Direction of the conjugate failure surface in relation to the logarithmic spiral.

Unlike the other theories which have used the logarithmic spiral failure surface, Rowe realized that the direction of the failure surface at the wall is determined by the roughness δ of the wall. In fact it was Terzaghi who apparently introduced the idea in his " Theoretical Soil Mechanics ", but he did not use it in the method attributed to him.

Figure 29 shows the condition at the bottom of the wall. The angle between the horizontal and the failure surface at the wall is α_w, which is considered to be positive when it is above the horizontal and negative when it is below the horizontal. In order to calculate the value of this angle for various soil friction angles, ϕ', and wall friction angles, δ, Mohr's circle of stresses may be used (figure 30)

From figure 30 :

$$AB = AP = \tfrac{1}{2}(\sigma_1 - \sigma_3)$$

$$<OAB = 90^\circ - \phi'$$

$$<ODA = 180^\circ - (90^\circ - \phi') - \delta = 90^\circ + \phi' - \delta$$

$$<BDP = <ODA = 90^\circ + \phi' - \delta$$

$$DBP = 180^\circ - (90^\circ + \phi' - \delta) - (\delta + \alpha_w) = 90^\circ - \phi' - \alpha_w$$

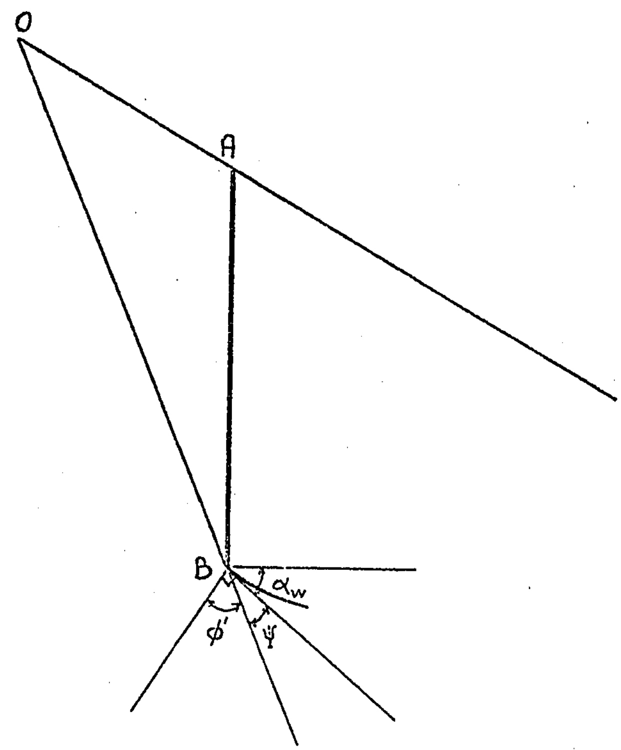

Figure 29. Failure surface condition at the bottom of the wall, Rowe's analysis.

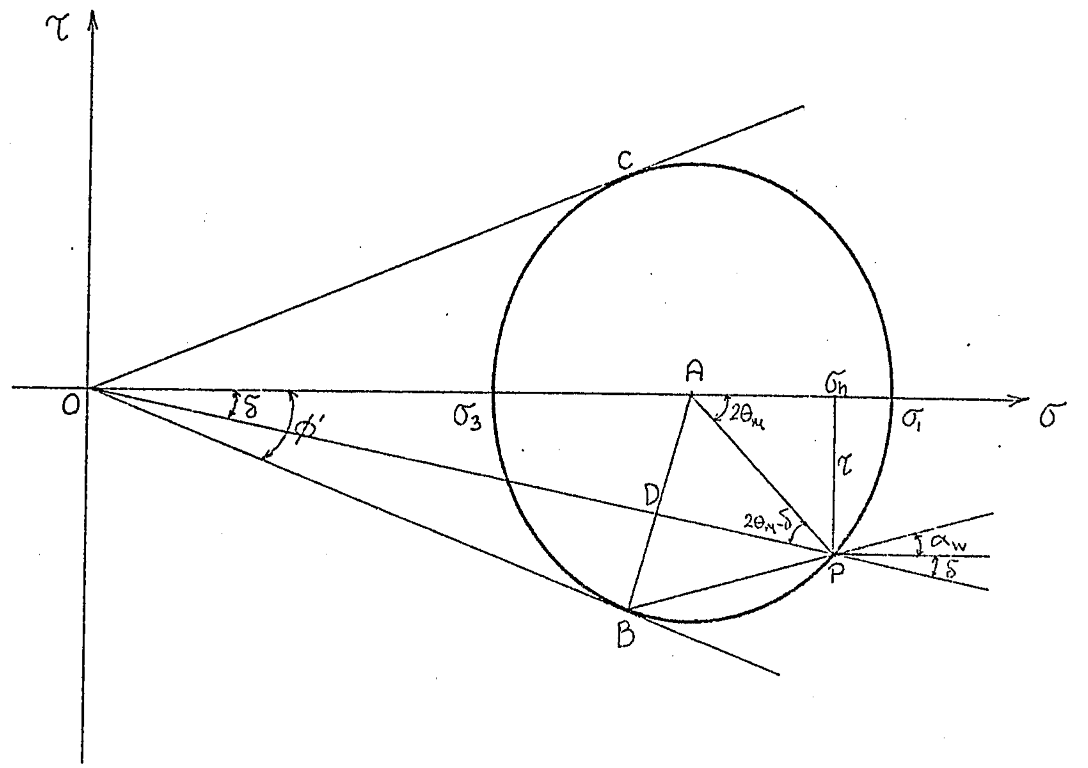

Figure 30. Mohr's circle of stresses for the condition at the bottom of the wall.

$$<APB = <ABP = <DBP = 90^{\circ}-\phi'-\alpha_{w}$$

$$<BAP = 180^{\circ}-2(90^{\circ}-\phi'-\alpha_{w}) = 2\phi'+2\alpha_{w} = 2(\phi'+\alpha_{w})$$

From triangle ABP, using the law of sines :

$$\frac{BP}{\sin <BAP} = \frac{AP}{\sin <ABP}$$

then,

$$\frac{BP}{\sin 2(\phi'+\alpha_{w})} = \frac{\frac{1}{2}(\sigma_{1}-\sigma_{3})}{\sin(90^{\circ}-\phi'-\alpha_{w})}$$

therefore,

$$BP = \tfrac{1}{2}(\sigma_{1}-\sigma_{3})\frac{\sin 2(\phi'+\alpha_{w})}{\sin(90^{\circ}-\phi'-\alpha_{w})}$$

from trigonometry :

$$\sin 2(\phi'+\alpha_{w}) = 2\sin(\phi'+\alpha_{w})\cos(\phi'+\alpha_{w})$$

$$\sin(90^{\circ}-\phi'-\alpha_{w}) = \sin\{90^{\circ}-(\phi'+\alpha_{w})\} = \cos(\phi'+\alpha_{w})$$

then,

$$BP = \tfrac{1}{2}(\sigma_{1}-\sigma_{3})\frac{2\sin(\phi'+\alpha_{w})\cos(\phi'+\alpha_{w})}{\cos(\phi'+\alpha_{w})}$$

therefore,

$$BP = (\sigma_1 - \sigma_3)\sin(\phi' + \alpha_w)$$

From triangle OAB :

$$OB = \tfrac{1}{2}(\sigma_1 - \sigma_3)/\tan\phi'$$

Considering triangle OPB, and applying the law of sines to it we obtain :

$$\frac{OB}{\sin \angle OPB} = \frac{BP}{\sin \angle POB}$$

therefore,

$$\frac{\tfrac{1}{2}(\sigma_1 - \sigma_3)/\tan\phi'}{\sin(\delta + \alpha_w)} = \frac{(\sigma_1 - \sigma_3)\sin(\phi' + \alpha_w)}{\sin(\phi' - \delta)}$$

$$\tfrac{1}{2}\sin(\phi' - \delta) = \sin(\phi' + \alpha_w)\sin(\delta + \alpha_w)\tan\phi'$$

from trigonometry :

$$\sin(\phi' + \alpha_w)\sin(\delta + \alpha_w) = \tfrac{1}{2}\cos(\phi' + \alpha_w - \delta - \alpha_w) - \tfrac{1}{2}\cos(\phi' + \alpha_w + \delta + \alpha_w)$$

then,

$$\frac{\frac{1}{2}\sin(\phi'-\delta)}{\tan\phi'} = \tfrac{1}{2}\cos(\phi'-\delta)-\tfrac{1}{2}\cos(\phi'+\delta+2\alpha_W)$$

$$\cos(\phi'+\delta+2\alpha_W) = \cos(\phi'-\delta)-\frac{\sin(\phi'-\delta)}{\tan\phi'}$$

$$(\phi'+\delta+2\alpha_W) = \text{Arccos}\{\cos(\phi'-\delta)-\frac{\sin(\phi'-\delta)}{\tan\phi'}\}$$

therefore,

$$\alpha_W = \tfrac{1}{2}\{\text{Arccos}[\cos(\phi'-\delta)-\frac{\sin(\phi'-\delta)}{\tan\phi'}]-\phi'-\delta\} \qquad (5.10)$$

The logarithmic spiral must leave the wall at an angle of α_W. To accommodate this, the ray from the center of the logarithmic spiral must intersect the failure surface at the wall at an angle Ψ (figure 31). The intersection of this ray with the conjugate failure surface (or its extension) defines precisely the location of the center of the logarithmic spiral, O.

In summation, considering the case with wall friction represented by the wall friction angle, δ, the following has been arrived at :

The soil wedge CDE is in a passive Rankine state (figure 31) and the value of the passive force acting on the soil height H_R is given by,

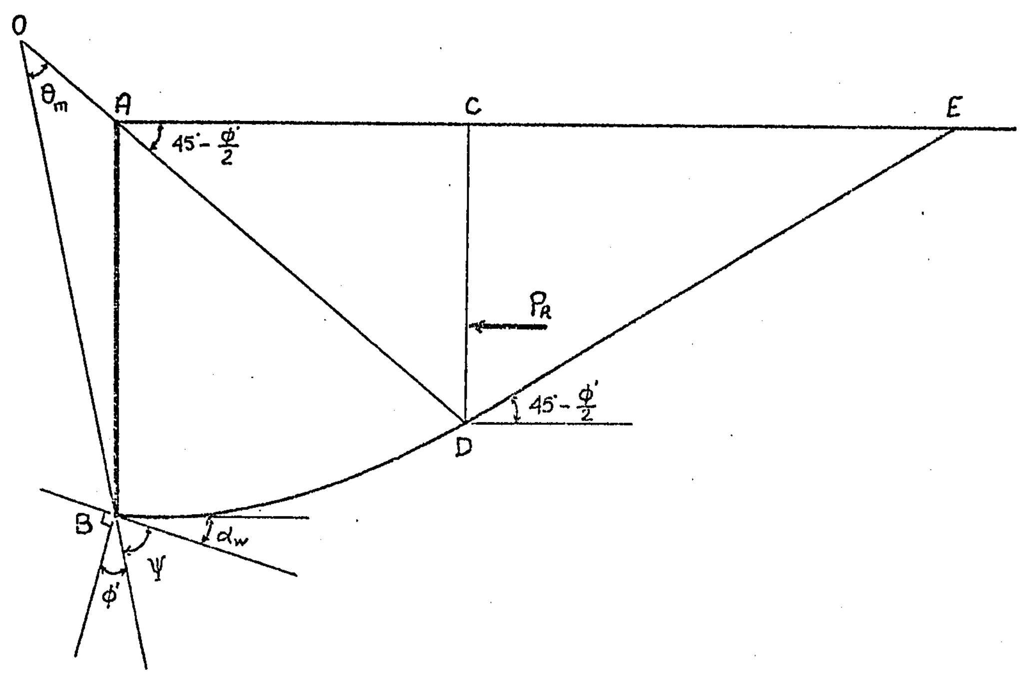

Figure 31. Rowe-Coulomb failure surface.

$$P_R = \tfrac{1}{2}\gamma H_R^2 \tan^2(45^{o}+\tfrac{1}{2}\phi')$$

From equation (5.2) the passive force created by ABCD is :

$$dE = \Sigma\{(W+dX)\tan(\alpha+\phi')\}$$

where Σ is taken in the zone ABCD. Therefore,

$$P_P = P_R+\Sigma\{(W+dX)\tan(\alpha+\phi')\} \qquad (5.11)$$

where,

$$X = 0 \text{ at CD} \quad \text{and} \quad X = P_p\tan\delta \text{ at the wall}$$

In order to find the distribution of the shear stresses it is necessary to assume the point of action of forces E and E+dE. Assuming E and E+dE act at the lower third points, since they are essentially gravitational stresses, the distribution of the shear stresses can be calculated as follows :

From figure 18,

$\Sigma M_n = 0$

$$(X+dX)(\tfrac{1}{2}b)+(X)(\tfrac{1}{2}b)-(E+dE)\{\tfrac{1}{3}(h+\tfrac{b}{2}\tan\alpha)-(\tfrac{1}{2}b)\tan\alpha\}$$
$$+E\{\tfrac{1}{3}(h-\tfrac{b}{2}\tan\alpha)+(\tfrac{1}{2}b)\tan\alpha\} = 0$$

$$(2X+dX)(\tfrac{1}{2}b)-(E+dE)(\frac{h}{3}-\frac{b}{3}\tan\alpha)+E(\frac{h}{3}+\frac{b}{3}\tan\alpha) = 0$$

dividing each term by b and rearranging,

$$X+\tfrac{1}{2}dX = \frac{Eh}{3b}-\frac{E}{3}\tan\alpha+\frac{h.dE}{3b}-\frac{dE}{3}\tan\alpha-\frac{Eh}{3b}-\frac{E}{3}\tan\alpha$$

therefore,

$$X+\tfrac{1}{2}dX = \frac{-2E}{3}\tan\alpha+\frac{dE}{3}(\frac{h}{b}-\tan\alpha) \qquad (5.12)$$

In order to solve for E and dE, figure 30 is considered again. From triangle OAP using the law of sines the following relation is obtained :

$$\frac{\sin\delta}{AP} = \frac{\sin(2\theta_m-\delta)}{OA}$$

therefore,

$$\frac{\sin\delta}{\tfrac{1}{2}(\sigma_1-\sigma_3)} = \frac{\sin(2\theta_m-\delta)}{\tfrac{1}{2}(\sigma_1+\sigma_3)}$$

$$\frac{\sin(2\theta_m-\delta)}{\sin\delta} = \frac{\sigma_1+\sigma_3}{\sigma_1-\sigma_3}$$

where,

$$\sin\phi' = \frac{AB}{OA} = \frac{\frac{1}{2}(\sigma_1-\sigma_3)}{\frac{1}{2}(\sigma_1+\sigma_3)} = \frac{\sigma_1-\sigma_3}{\sigma_1+\sigma_3}$$

let $J = 1/\sin\phi'$, then

$$\frac{\sin(2\theta_m-\delta)}{\sin\delta} = J$$

$$J.\sin\delta = \sin(2\theta_m-\delta)$$

from trigonometry,

$$\sin(2\theta_m-\delta) = \sin2\theta_m\cos\delta-\cos2\theta_m\sin\delta$$

then,

$$J = \frac{\sin2\theta_m}{\tan\delta} - \cos2\theta_m$$

therefore,

$$\tan\delta = \frac{\sin2\theta_m}{J+\cos2\theta_m}$$

but,

$$\tan\delta = \frac{X+dX}{E+dE} \quad \text{at the wall}$$

therefore,

$$E+dE = (X+dX)\left(\frac{J+\cos2\theta_m}{\sin2\theta_m}\right) \tag{5.13}$$

Differentiating equation (5.13) with respect to θ_m and neglecting second degree differential terms :

$$\frac{dE}{d\theta_m} = \left(\frac{J+\cos 2\theta_m}{\sin 2\theta_m}\right)\frac{dX}{d\theta_m} - \frac{2X}{\sin^2 2\theta_m}(J\cos 2\theta_m+1) - \frac{2dX}{\sin^2 2\theta_m}(J\cos 2\theta_m+1)$$

$$dE = \left(\frac{J+\cos 2\theta_m}{\sin 2\theta_m}\right)dX - X\left\{\frac{2}{\sin^2 2\theta_m}(J\cos 2\theta_m+1)\right\}d\theta_m \tag{5.14}$$

Substituting equations (5.13) and (5.14) into equation (5.12)

$$X+\tfrac{1}{2}dX = \left(-\frac{2}{3}\tan\alpha\right)\left\{(X+dX)\left(\frac{J+\cos 2\theta_m}{\sin 2\theta_m}\right) - \left(\frac{J+\cos 2\theta_m}{\sin 2\theta_m}\right)dX\right.$$

$$\left. + \frac{2X}{\sin^2 2\theta_m}(J\cos 2\theta_m+1)\,d\theta_m\right\}$$

$$+\frac{1}{3}\left(\frac{h}{b}-\tan\alpha\right)\left\{\left(\frac{J+\cos 2\theta_m}{\sin 2\theta_m}\right)dX - \frac{2X}{\sin^2 2\theta_m}(J\cos 2\theta_m+1)\,d\theta_m\right\}$$

multiplying each term by (2/X) and simplifying :

$$\frac{dX}{X} - \frac{2}{3}\frac{dX}{X}\left(\frac{J+\cos 2\theta_m}{\sin 2\theta_m}\right)\left(\frac{h}{b}-\tan\alpha\right) = -2-\frac{4\tan\alpha}{3\sin 2\theta_m}(J+\cos 2\theta_m)$$

$$-\frac{4}{3}\left(\frac{J\cos 2\theta_m+1}{\sin^2 2\theta_m}\right)\left(\frac{h}{b}-\tan\alpha\right)d\theta_m$$

therefore,

$$\frac{dX}{X} = \frac{2\{1+\frac{2}{3}(\frac{J+\cos 2\theta_m}{\sin 2\theta_m})\tan\alpha+\frac{2}{3}(\frac{h}{b}-\tan\alpha)(\frac{J.\cos 2\theta_m+1}{\sin^2 2\theta_m})d\theta_m\}}{-1+\frac{2}{3}(\frac{h}{b}-\tan\alpha)(\frac{J}{\sin 2\theta_m}+\cot 2\theta_m)} \qquad (5.15)$$

Using equation (5.15) the change in the vertical shear force across a slice may be calculated. Thus, the vertical shear force between any two slices can be calculated as a percentage of the vertical shear force at the wall. This force at the wall is defined by P_p and δ.

While the foregoing may be considered to be a 'rigorous' solution to the earth pressure problem, the importance of the assumption that the horizontal inter-slice forces act at the lower third point has not been tested. Concessibly, other, lower values of K_p will result if the horizontal forces are considered to act at some other height relative to the height of the slice. In fact the relative height may not be a constant but could vary from slice to slice. An infinite number of possibilities opens up.

Rowe suggested that the lowest values of K_p will result if it is assumed that all the vertical shear forces are lost close to the wall where the shear forces, X, are the greatest. Therefore dX=0 except for the slice closest to the wall where $dX=X_{wall}$. The shear force across a slice, dX, may be thought of as an increase in the weight of the slice. Concentrating dX close to the wall means in effect that all this "weight" is concentrated in this slice. Since the slice closest to the wall has to be pushed along a failure plane with the minimum (or even negative) angle α, this "weight" is easier to move than if it were pushed up some steeper angle further from the wall.

From equation (5.11) :

$$P_p = P_R + \Sigma\{W.\tan(\alpha+\phi') + dX.\tan(\alpha+\phi')\}$$

at the wall, $\alpha=\alpha_w$ and $dX=P_p.\tan\delta$. Then,

$$P_p = P_R + \Sigma\{W.\tan(\alpha+\phi')\} + P_p.\tan\delta.\tan(\alpha_w+\phi')$$

therefore,

$$P_p = \frac{P_R + \Sigma\{W.\tan(\alpha+\phi')\}}{1-\tan\delta.\tan(\alpha_w+\phi')} \qquad (5.16)$$

but,

$$P_p = \tfrac{1}{2}\gamma H^2 K_p \quad ,$$

therefore,

$$K_p = \frac{P_R + \Sigma\{W.\tan(\alpha+\phi')\}}{1-\tan\delta.\tan(\alpha_w+\phi')} \left(\frac{2}{\gamma H^2}\right) \qquad (5.17)$$

By assuming that all vertical shear is lost at or close to the wall, a very simple expression for K_p has been derived. It is this expression that forms the Rowe-Coulomb method.

PART III. FINDINGS

CHAPTER 6. CALCULATIONS AND RESULTS

CHAPTER 7. COMPARISON OF RESULTS AND DISCUSSION

CHAPTER 8. CONCLUSION AND RECOMMENDATIONS FOR FURTHER WORK

CHAPTER 6. CALCULATIONS AND RESULTS

No published values for K_p based on the Rowe-Coulomb method, either rigorous or simplified, are available. The intent of this thesis was to calculate values of K_p for the special case of a vertical, rigid, rough wall retaining ideal, dry sand with horizontal ground surface.

In order to calculate the values of K_p for varying ϕ' and δ angles using the Rowe-Coulomb method, first the failure surface is established.

A computer program is prepared in FORTRAN IV language in order to calculate the values of α_w from equation (5.10) for varying values of ϕ' and δ. Internal friction angle, ϕ', varies from 20^o up to 45^o and the wall friction angle, δ, is increased in 1^o increments from 1^o to $\delta=\phi'$.

A part of the program (for $\phi'=40^o$) is given below and the results obtained for α_w are tabulated in figure 32. In this figure only the values of α_w for 5^o increments of δ are shown because K_p values are calculated for these increments.

```
A=3.14159/180.0
AA=0.5
ED=40.0
CZ=1.0
```

Figure 32

ϕ' (degrees)	δ (degrees)	α_w (radians)	α_w (degrees)
20	5	+0.44	+25.12
	10	+0.26	+14.74
	15	+0.05	+ 2.91
	20	-0.35	-20.00
25	5	+0.42	+24.05
	10	+0.27	+15.37
	15	+0.11	+ 6.12
	20	-0.08	- 4.51
	25	-0.44	-25.00
30	5	+0.39	+22.48
	10	+0.26	+14.84
	15	+0.12	+ 6.91
	20	-0.03	- 1.58
	25	-0.20	-11.35
	30	-0.52	-30.00
35	5	+0.36	+20.63
	10	+0.24	+13.69
	15	+0.11	+ 6.59
	20	-0.01	- 0.80

cont.

ϕ' (degrees)	δ (degrees)	α_w (radians)	α_w (degrees)
35	25	-0.15	- 8.73
	30	-0.31	-17.83
	35	-0.61	-35.00
40	5	+0.32	+18.60
	10	+0.21	+12.16
	15	+0.10	+ 5.63
	20	-0.02	- 1.07
	25	-0.14	- 8.05
	30	-0.27	-15.53
	35	-0.42	-24.08
	40	-0.70	-40.00
45	5	+0.29	+16.46
	10	+0.18	+10.39
	15	+0.07	+ 4.26
	20	-0.03	- 1.96
	25	-0.15	- 8.35
	30	-0.26	-15.00
	35	-0.39	-22.10
	40	-0.53	-30.19
	45	-0.79	-45.00

Figure 32. α_w values for varying ϕ' and δ angles.

```
      EA=0.8391
      DO  31   I=1,40
      ALFAW=AA×(ARCOS(COS(A×(ED-CZ))
           -SIN(A×(ED-CZ))/EA)-(A×(ED+CZ)))
      ANGLE=ALFAW/A
      WRITE (3,101)  CZ,ALFAW,ANGLE
   31 CZ=CZ+1.0
      RETURN
      END
```

Additional geometric relationships are required to describe the failure surface. The relation between the angle of the logarithmic spiral, θ_m, and the angles ϕ' and α_w is given below :

From figure 31,

$$<ABO = 90^{o}-(\Psi-\alpha_w)$$

(α_w being negative)

where,

$$\Psi = 90^{o}-\phi'$$

therefore,

$$<ABO = \phi'+\alpha_w$$

Considering triangle OAB ;

$$\theta_m = 180^\circ - (135^\circ - \tfrac{1}{2}\phi') - (\phi' + \alpha_w)$$

therefore,

$$\theta_m = 45^\circ - \tfrac{1}{2}\phi' - \alpha_w \qquad (6.1)$$

The following relationships will hold for the failure surface as described. Reference is made to figure 33.

Let $H = 10.0$

$OB = r_o$

$OP = r_\theta = r_o e^{\theta.\tan\phi'} \qquad (5.3)$

$OD = r_m = r_o e^{\theta_m \tan\phi'}$

$AC = CE$

$<BOP = \theta$

$<BOA = \theta_m = 45^\circ - \tfrac{1}{2}\phi' - \alpha_w \qquad (6.1)$

$<OAB = 135^\circ - \tfrac{1}{2}\phi'$

$<ABO = 45^\circ + \tfrac{1}{2}\phi' - \theta_m$

$<DAC = 45^\circ - \tfrac{1}{2}\phi'$

from triangle OAB :

$$\frac{OB}{\sin <OAB} = \frac{AB}{\sin <BOA}$$

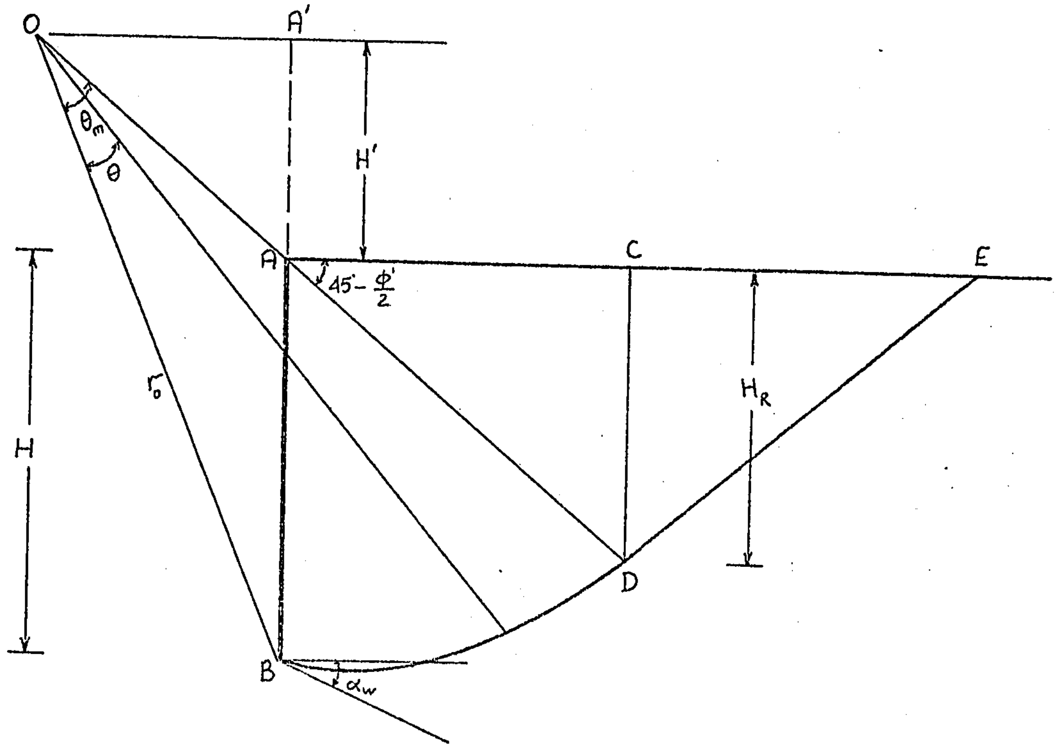

Figure 33. Relationships describing the Rowe-Coulomb failure surface.

$$\frac{r_o}{\sin(135^{\circ}-\frac{1}{2}\phi')} = \frac{10.0}{\sin\theta_m}$$

$$r_0 = 10.0\frac{\sin(135^{\circ}-\frac{1}{2}\phi')}{\sin\theta_m}$$

therefore,

$$r_o = 10.0\frac{\sin(45^{\circ}+\frac{1}{2}\phi')}{\sin\theta_m} \tag{6.2}$$

Once again using the law of sines for the same triangle OAB :

$$\frac{OA}{\sin <ABO} = \frac{AB}{\sin <BOA}$$

let OA = a, then

$$\frac{a}{\sin(45^{\circ}+\frac{1}{2}\phi'-\theta_m)} = \frac{10.0}{\sin\theta_m}$$

therefore,

$$a = 10.0\frac{\text{Sin}(45^{\circ}+\frac{1}{2}\phi'-\theta_m)}{\sin\theta_m} \tag{6.3}$$

Also from triangle ADC :

$$CD = H_R = \overline{AD}.\sin(45^{\circ}-\tfrac{1}{2}\phi')$$

$$= (OD-OA)\sin(45^{\circ}-\tfrac{1}{2}\phi')$$

therefore,

$$H_R = (r_{\theta_m}-a)\sin(45^{\circ}-\tfrac{1}{2}\phi') \qquad (6.4)$$

Additional relations are :

$$H' = a.\sin(45^{\circ}-\tfrac{1}{2}\phi') \qquad (6.5)$$

and

$$OA' = \frac{H'}{\tan(45^{\circ}-\tfrac{1}{2}\phi')} \qquad (6.6)$$

The variation of the value of angle α on the failure surface may be shown as follows (figure 34) :

$$\lambda = 45^{\circ}-\tfrac{1}{2}\phi'+\theta_m-\theta$$

also,

$$\lambda+\phi'+\alpha = 90^{\circ}$$

$$\alpha = 90^{\circ}-\phi'-\lambda$$

then,

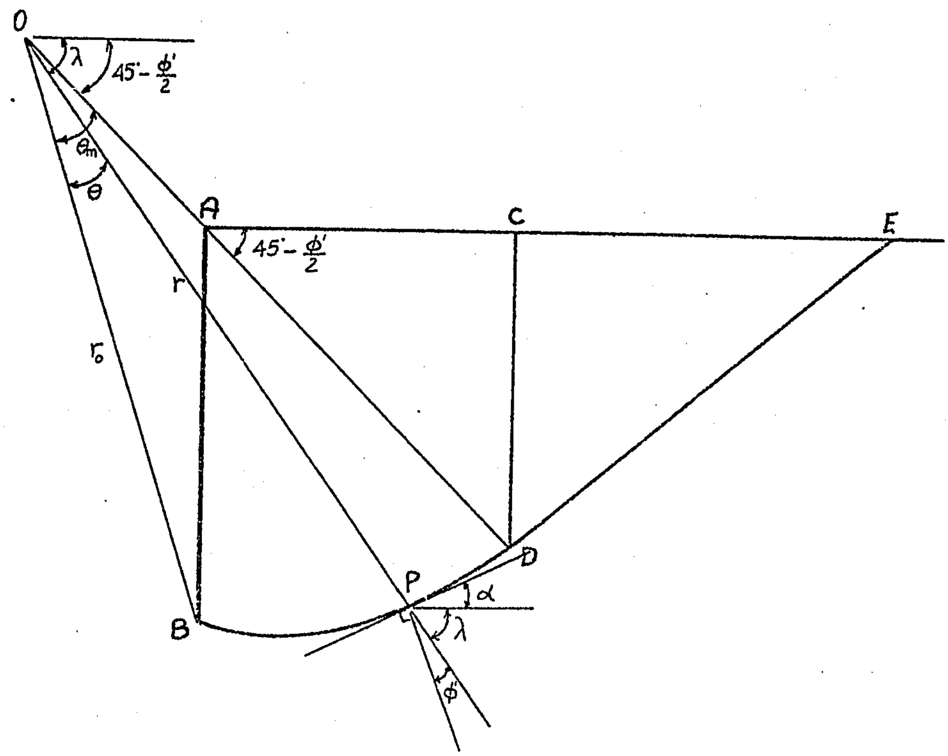

Figure 34. Variation of α on the failure surface.

$$\alpha = 90^{o}-\phi'-(45^{o}-\tfrac{1}{2}\phi'+\theta_{m}-\theta)$$

$$\alpha = 45^{o}-\tfrac{1}{2}\phi'-\theta_{m}+\theta$$

but

$$45^{o}-\tfrac{1}{2}\phi'-\theta_{m} = \alpha_{w} \tag{6.1}$$

therefore,

$$\alpha = \alpha_{w}+\theta \tag{6.7}$$

Assuming that all the shear is lost at the wall the logarithmic spiral part of the failure region is divided into vertical slices by varying the angle θ, 1^{o} at a time. In order to calculate the coefficient of passive earth pressure, K_p, equation (5.18) is used and to facilitate the calculations a computer program in FØRTRAN IV language is written.

The slice area is considered to be a trapezoid and the angle of the failure surface, α, is taken as the average value of the angles at either side of the slice.

The program will calculate for each slice, the product of the slice area and the value $\tan(\phi'+\alpha)$. If the last slice has an angle $\theta<1^{o}$ then for this particular slice the product is calculated separately with an electric calculator. The calculator is also used to sum up these values for all the slices.

A sample program for ($\phi'=40^{\circ}$, $\delta=20^{\circ}$) is shown below and the K_p values obtained are given in figure 35 for values of ϕ' ranging from 20° to 45° in 5° intervals and δ ranging from 0° to ϕ' in 5° intervals. Figure 36 gives these values in a graphical form.

```
H=25.0
A=3.14159/180.0
QQ=-0.018733
DC=10.0
UU=65.0
CU=0.8391
CZ=1.0
DB=2.0
AC=40.0
B=0.5
BA=0.0
DO  141   I=1,26
TETAM=H×A-QQ
RZERO=DC×SIN(A×UU)/SIN(TETAM)
RTETM=RZERO×EXP(TETAM×CU)
ALNGT=DC×SIN(A×UU-TETAM)/SIN(TETAM)
HRANK=(RTETM-ALNGT)×SIN(A×H)
HPRIM=ALNGT×SIN(A×H)
SZEK=SIN(TETAM+A×(H-BA))
```

Figure 35

ϕ' (degrees)	δ (degrees)	K_p
20	0	2.04
	5	2.26
	10	2.43
	15	2.55
	20	2.70
25	0	2.46
	5	2.77
	10	3.03
	15	3.23
	20	3.39
	25	3.63
30	0	3.00
	5	3.43
	10	3.80
	15	4.13
	20	4.40
	25	4.64
	30	5.03

cont.

Figure 35

ϕ' (degrees)	δ (degrees)	K_p
35	0	3.69
	5	4.29
	10	4.84
	15	5.34
	20	5.80
	25	6.21
	30	6.59
	35	7.25
40	0	4.60
	5	5.44
	10	6.26
	15	7.05
	20	7.80
	25	8.51
	30	9.18
	35	9.83
	40	11.03

cont.

ϕ' (degrees)	δ (degrees)	K_p
45	0	5.83
	5	7.06
	10	8.30
	15	9.55
	20	10.80
	25	12.04
	30	13.26
	35	14.46
	40	15.69
	45	18.01

Figure 35. Values of K_p for varying ϕ' and δ angles given by the Rowe-Coulomb method.

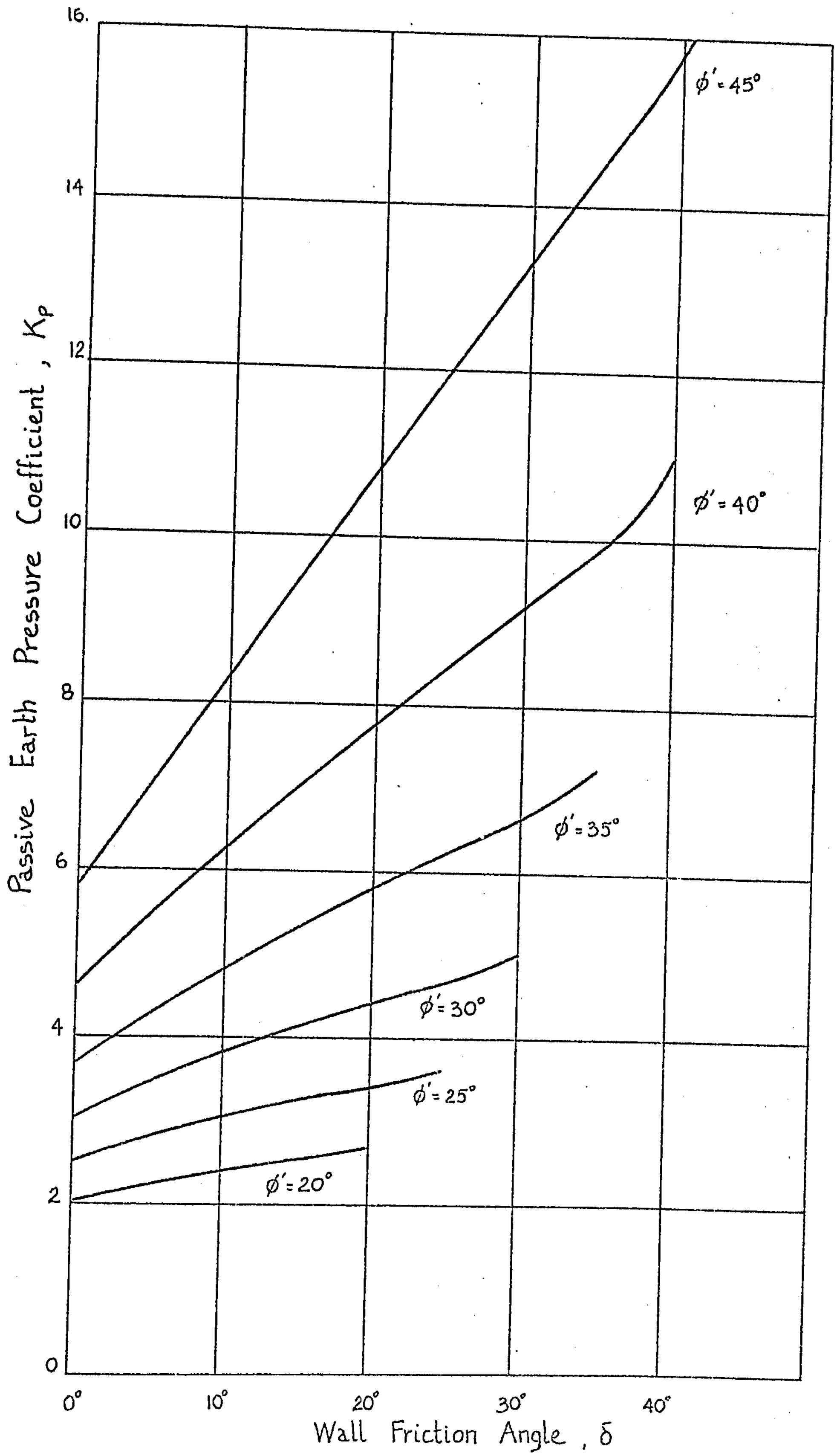

Figure 36. K_p values for dry, cohesionless soil behind a rough vertical wall with horizontal ground surface - Rowe-Coulomb method.

```
      SCAR=SIN(TETAM+A×(H-BA-CZ))
      HONE=RZERO×EXP(A×BA×CU)×SZEK-HPRIM
      HTWO=RZERO×EXP(A×(BA+CZ)×CU)×SCAR-HPRIM
      CZEK=COS(TETAM+A×(H-BA))
      CCAR=COS(TETAM+A×(H-BA-CZ))
      BVAR=RZERO×(EXP(A×(BA+CZ)×CU)×CCAR
     1     -EXP(A×BA×CU)×CZEK)
      AREA=(HONE+HTWO)×BVAR/DB
      TALFA=TAN(A×(AC+B+BA)+QQ)
      GOAL=AREA×TALFA
141   BA=BA+1.0
```

Values of K_p using the rigorous solution considering the shear forces on the slices are obtained for the cases ($\phi'=30^o$, $\delta=20^o$) and ($\phi'=40^o$, $\delta=30^o$), in order to compare with the results obtained assuming that all the shear is lost at the wall. The calculations for ($\phi'=40^o$, $\delta=30^o$) are given below. The failure surface and its properties are shown in figure 37.

Applying equation (5.15) to slices which are formed by varying the logarithmic spiral angle, θ, 5^o at a time we obtain :

α (deg.)	-13.0	-8.0	-3.0	+2.0	+7.0	+12.0	+17.0	+22.0	+24.75
θ (deg.)	38.0	33.0	28.0	23.0	18.0	13.0	8.0	3.0	0.25
h (ft.)	10.19	10.49	10.67	10.68	10.51	10.13	9.51	8.62	8.04
b (ft.)	1.60	1.75	1.90	2.05	2.19	2.32	2.45	2.55	0.28

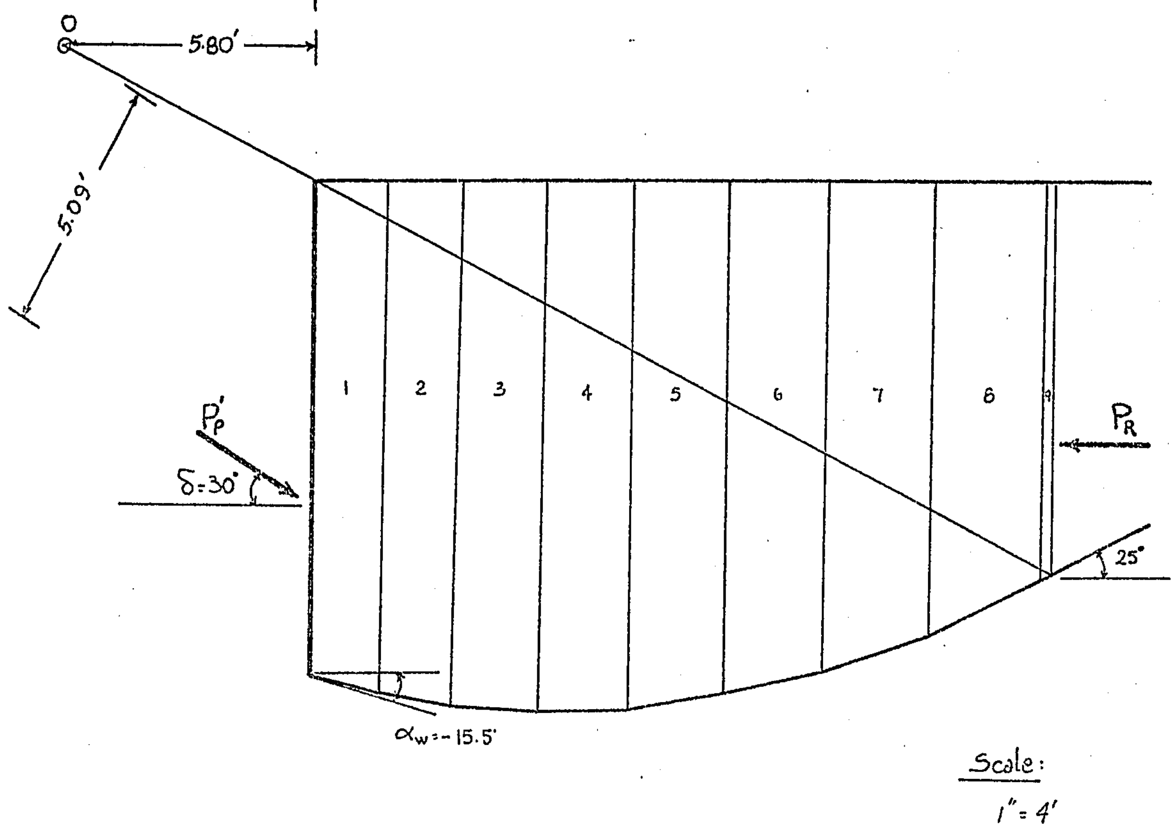

Figure 37. Failure surface and its properties for ($\phi'=40^{o}$, $\delta=30^{o}$), Rowe-Coulomb rigorous solution.

Slice #1

$$\frac{dX}{X} = \frac{2\{1+\frac{2}{3}(1.854)(-0.231)+\frac{2}{3}(6.586)(1.461)(0.087)\}}{-1+\frac{2}{3}(6.586)(1.853)} = 0.358$$

Slice #2

$$\frac{dX}{X} = \frac{2\{1+\frac{2}{3}(2.140)(-0.141)+\frac{2}{3}(6.141)(1.963)(0.087)\}}{-1+\frac{2}{3}(6.141)(2.149)} = 0.384$$

Slice #3

$$\frac{dX}{X} = \frac{2\{1+\frac{2}{3}(2.548)(-0.052)+\frac{2}{3}(5.662)(2.720)(0.087)\}}{-1+\frac{2}{3}(5.662)(2.553)} = 0.418$$

Slice #4

$$\frac{dX}{X} = \frac{2\{1+\frac{2}{3}(3.123)(+0.035)+\frac{2}{3}(5.165)(4.015)(0.087)\}}{-1+\frac{2}{3}(5.165)(3.127)} = 0.466$$

Slice #5

$$\frac{dX}{X} = \frac{2\{1+\frac{2}{3}(4.030)(+0.123)+\frac{2}{3}(4.677)(6.550)(0.087)\}}{-1+\frac{2}{3}(4.677)(4.018)} = 0.539$$

Slice #6

$$\frac{dX}{X} = \frac{2\{1+\frac{2}{3}(5.600)(+0.213)+\frac{2}{3}(4.157)(12.57)(0.087)\}}{-1+\frac{2}{3}(4.157)(5.600)} = 0.667$$

Slice #7

$$\frac{dX}{X} = \frac{2\{1+\frac{2}{3}(9.140)(+0.306)+\frac{2}{3}(3.574)(32.84)(0.087)\}}{-1+\frac{2}{3}(3.574)(9.140)} = 0.931$$

Slice #8

$$\frac{dX}{X} = \frac{2\{1+\frac{2}{3}(24.40)(+0.404)+\frac{2}{3}(2.976)(244.0)(0.087)\}}{-1+\frac{2}{3}(2.976)(24.40)} = 2.085$$

Slice #9

$$\frac{dX}{X} = \frac{2\{1+\frac{2}{3}(294.0)(+0.461)+\frac{2}{3}(28.26)(33780)(.0087)\}}{-1+\frac{2}{3}(28.26)(294.0)} = 2.040$$

Let $d\overline{X}$ = the shear change across a slice, if

$X+dX=\overline{X}=1.000$ at the wall.

The vertical shear force $\overline{X}_{12}$ between slices 1 and 2 becomes :

$$\overline{X}_{12} = \overline{X}_{wall} - d\overline{X}_{slice_1}$$

where,

$$d\overline{X}_{slice_1} = (\overline{X}_{wall})\left(\frac{dX}{X+dX}\right)_{slice_1} = (\overline{X}_{wall})\left(\frac{\frac{dX}{X}}{1+\frac{dX}{X}}\right)_{slice_1}$$

Similarly, the vertical shear force $\overline{X}_{23}$ between slices 2 and 3 is :

$$\bar{X}_{23} = \bar{X}_{12} - d\bar{X}_{slice_2}$$

where,

$$d\bar{X}_{slice_2} = (\bar{X}_{12})\left(\frac{\frac{dX}{X}}{1+\frac{dX}{X}}\right)_{slice_2}$$

Continuing in this fashion, the value of $d\bar{X}$ for each slice may be computed.

In reality, the value of (X+dX) at the wall is equal to ($P_p \tan\delta$), therefore the value of dX for any slice is $P_p \tan\delta . d\bar{X}$.

Now equation (5.11) which states :

$$P_p = P_R + \Sigma\{(W+dX)\tan(\alpha+\phi')\}$$

may be written :

$$P_p = P_R + \Sigma\{W.\tan(\alpha+\phi') + P_p \tan\delta . d\bar{X}.\tan(\alpha+\phi')\}$$

$$P_p = P_R + \Sigma\{W.\tan(\alpha+\phi')\} + P_p \tan\delta . \Sigma\{d\bar{X}.\tan(\alpha+\phi')\}$$

$$P_p\{1-\tan\delta . \Sigma[d\bar{X}.\tan(\alpha+\phi')]\} = P_R + \Sigma\{W.\tan(\alpha+\phi')\}$$

therefore,

$$P_p = \frac{P_R + \Sigma\{W.\tan(\alpha+\phi')\}}{1-\tan\delta . \Sigma\{d\bar{X}.\tan(\alpha+\phi')\}}$$

where,

$$P_R = \tfrac{1}{2}\gamma H_R^2 \tan^2(45^\circ + \tfrac{1}{2}\phi')$$

Substituting the values for the case ($\phi'=40^\circ$, $\delta=30^\circ$) into the derived expressions, the value of K_p' will be obtained. The calculations related to the shear change across slices are given in a tabular form on pages 89 and 90.

$$P_R = \tfrac{1}{2}\gamma(7.977)^2(4.6) = 146.33\gamma$$

$$\Sigma\{W.\tan(\alpha+\phi')\} = 191.57\gamma$$

$$\tan\delta = \tan 30^\circ = 0.5774$$

$$\Sigma\{d\overline{X}.\tan(\alpha+\phi')\} = 0.8322$$

therefore,

$$P_p = \frac{146.33\gamma+191.57\gamma}{1-(0.5774)(0.8322)} = \frac{337.90\gamma}{0.520}$$

On the other hand,

$$P_p = \tfrac{1}{2}\gamma H^2 K_p$$

then,

$$\tfrac{1}{2}\gamma(100)K_p = \frac{337.90\gamma}{0.520}$$

$$K_p = 13.0$$

Slice #	$\overline{X}$	dX/X	$\frac{dX/X}{1+(dX/X)}$	$d\overline{X}$
1	1.000	0.358	0.264	0.264
2	0.736	0.384	0.278	0.204
3	0.532	0.418	0.295	0.157
4	0.375	0.466	0.318	0.119
5	0.256	0.539	0.350	0.0896
6	0.1664	0.667	0.398	0.0663
7	0.1001	0.931	0.482	0.0483
8	0.0518	2.085	0.675	0.0350
9	0.0168	2.040	0.670	0.0113
	0.0055			

Slice #	Area=A	$\tan(\alpha+\phi')=T$	A.T	$d\overline{X}$	$T.d\overline{X}$
1	16.30	0.5095	8.30	0.264	0.1344
2	18.36	0.6249	11.47	0.204	0.1273
3	20.27	0.7536	15.35	0.157	0.1181
4	21.89	0.9004	19.71	0.119	0.1070
5	23.02	1.0724	24.68	0.090	0.0964
6	23.50	1.2799	30.10	0.066	0.0848
7	23.30	1.5399	35.82	0.048	0.0743
8	21.98	1.8807	41.36	0.035	0.0659
9	2.25	2.1234	4.78	0.011	0.0240
			$\Sigma=191.57\ ft^2$		$\Sigma=0.8322$

CHAPTER 7. COMPARISON OF RESULTS AND DISCUSSION

After reviewing the theoretical and experimental works on the passive earth pressure problem, the Rowe-Coulomb method is introduced and values for K_p are calculated. These studies and the K_p values obtained are discussed below :

i) Discussion on the Rowe-Coulomb method.

a. Slice thickness :

In order to investigate the effect of the slice width on the calculations the value of K_p is calculated for various $\Delta\theta$ values using two cases. The results are shown below,

	θ (degrees)			
	0.5	1.0	2.0	5.0
($\phi'=35°$, $\delta=30°$)		6.59		6.58
($\phi'=40°$, $\delta=30°$)	9.18	9.18	9.18	

These results indicate that the calculations are insensitive to slice thickness, at least within the range of rational widths used.

b. Rigorous analysis versus the Rowe-Coulomb method :

Rowe indicated that the minimum value of K_p will result if all the shear is assumed to be lost at the wall. To see the difference between (1) the K_p values obtained by considering the vertical shear forces to be distributed among a number of slices and (2) by assuming this shear force to be present only at the wall, two cases are solved using both methods. Calculated values of K_p are shown below,

	($\phi'=40°, \delta=30°$)	($\phi'=30°, \delta=20°$)
(1) Rigorous solution	13.0	5.2
(2) Rowe-Coulomb method	9.2	4.4

Comparison of these values shows that the simplifying assumption of a total shear loss near the wall does lead to lower values of K_p. The values obtained by the Rowe-Coulomb method will lead in most instances to safer design.

It should be kept in mind that even with the rigorous method simplifying assumptions are made concerning the location of the resultant forces on the sides of the slices. Changing the position and distribution of the location of resultant forces could lead to different values of K_p.

ii) Comparison between Rowe-Coulomb and Janbu's methods.

The Rowe-Coulomb method is basically the same as Janbu's slice method. Both of these methods start by considering the forces acting on a slice and write the equilibrium equations of the slice. There are, however, some differences between the two methods.

a. Distribution of vertical shear :

The distribution of vertical shear among the slices in Janbu's method is obtained by successive approximations. The Rowe-Coulomb method on the other hand assumes that vertical shear exists in only the slice closest to the wall.

b. Failure surface :

One advantage of the Rowe-Coulomb method is that the failure surface is set at the beginning of the analysis. With Janbu's method one has to investigate the minimum value of K_p by successive alterations to the shape of the logarithmic spiral failure surface.

For comparison purposes, values obtained for K_p using these two methods are plotted together in figure 38. The Rowe-Coulomb method gives consistently lower values for K_p than Janbu's method and therefore leads to safer design. It should be noted, however, that the rigorous solution, being limited to one predetermined, kinematically acceptable failure surface, gives higher K_p values than Janbu's method.

c. Varying soil constants :

Janbu's method fails to give results on the safer side compared to other well known theories for simple cases. When variable soil constants and pore water pressures are involved in the problem, Janbu's slice method proves to be very useful. The Rowe-Coulomb method can also be modified to include these complicated cases.

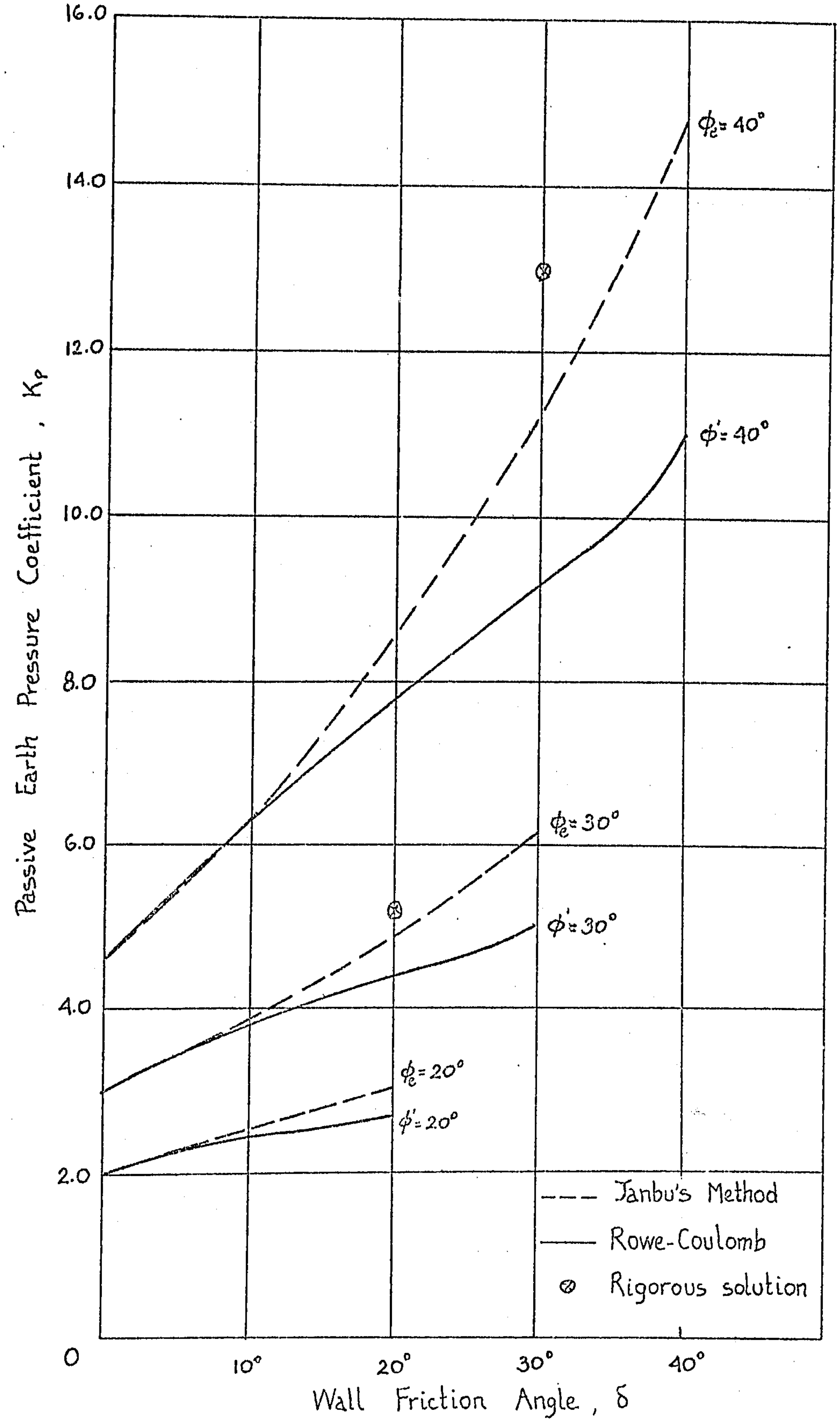

Figure 38. Comparison of K_p values obtained by the Rowe-Coulomb method with Janbu's results.

iii) Rowe-Coulomb method as compared to other methods.

K_p values for two different ϕ' angles, 40° and 30°, and varying δ angles are plotted in figures 39 and 40. From these figures it is noted again that the rigorous solution gives values of K_p higher than the other theories. The Rowe-Coulomb method itself gives lower K_p values than these other known theories. Thus, the Rowe-Coulomb method is safer than any of the other known theories for most design cases. There are, however, recent theories investigating the values of K_p for different wall movements. Graham's calculations, for example, gives promise of producing K_p values which are in fair agreement with experimental results over a wide range of soil densities, but more research has to be done on the subject before full confidence can be placed in this method (4).

iv) Comparison of the Rowe-Coulomb values of K_p with experimental data.

Experimental values given by Rowe and Peaker (1965) and also of Narain et al (1969) for K_p are compared with the Rowe-Coulomb values in figure 41. Peaker's tests in 1964 were conducted with wall translation only. The values given for Narain et al are also for wall translation. The properties of the sands used in these experiments are shown below :

Peaker's experiments,

loose density = 93 lbs/cu.ft.

dense density = 103 lbs/cu.ft.

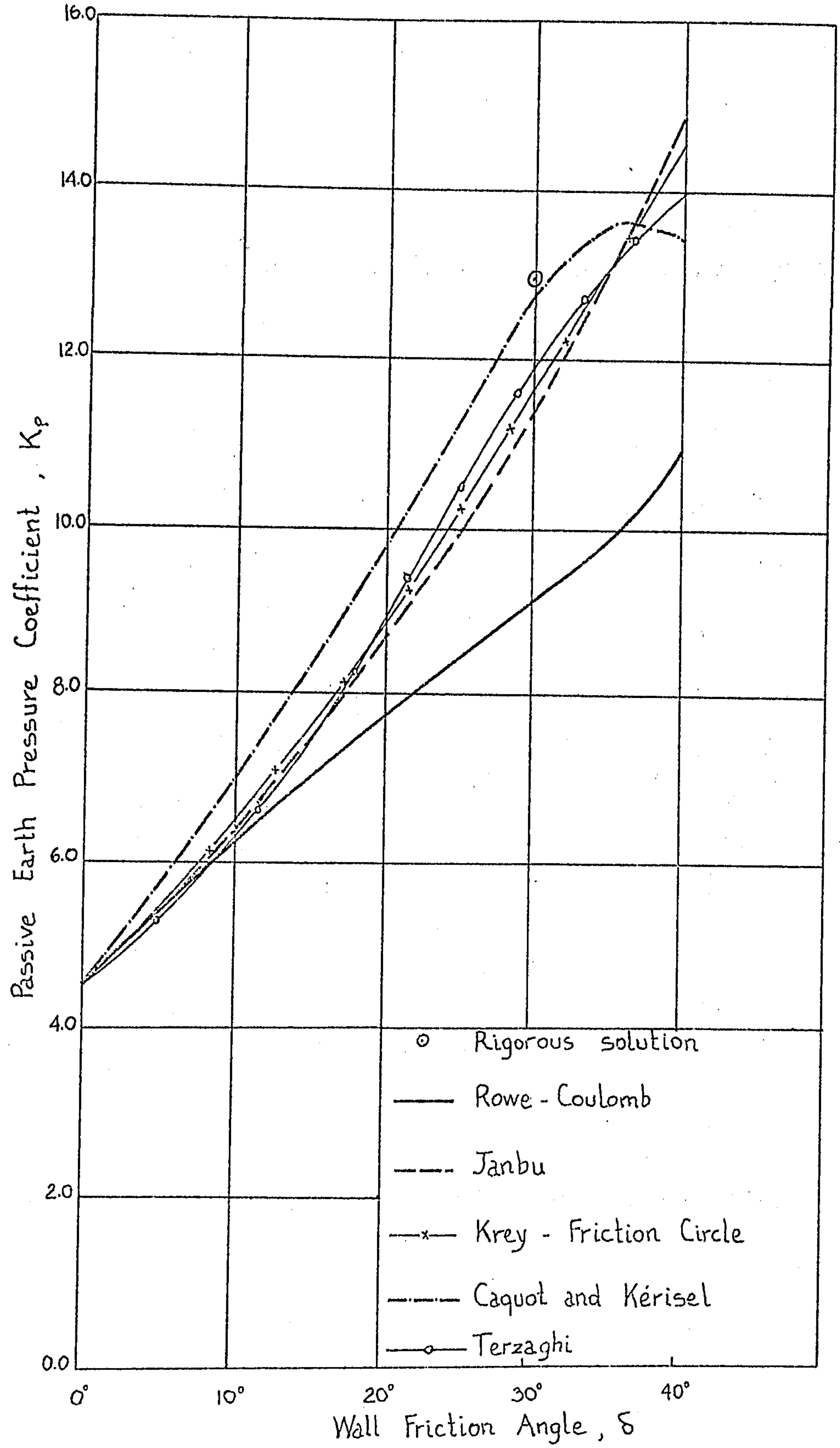

Figure 39. Comparison of Rowe-Coulomb values of K_p with other theories for $\phi'=40^{\circ}$.

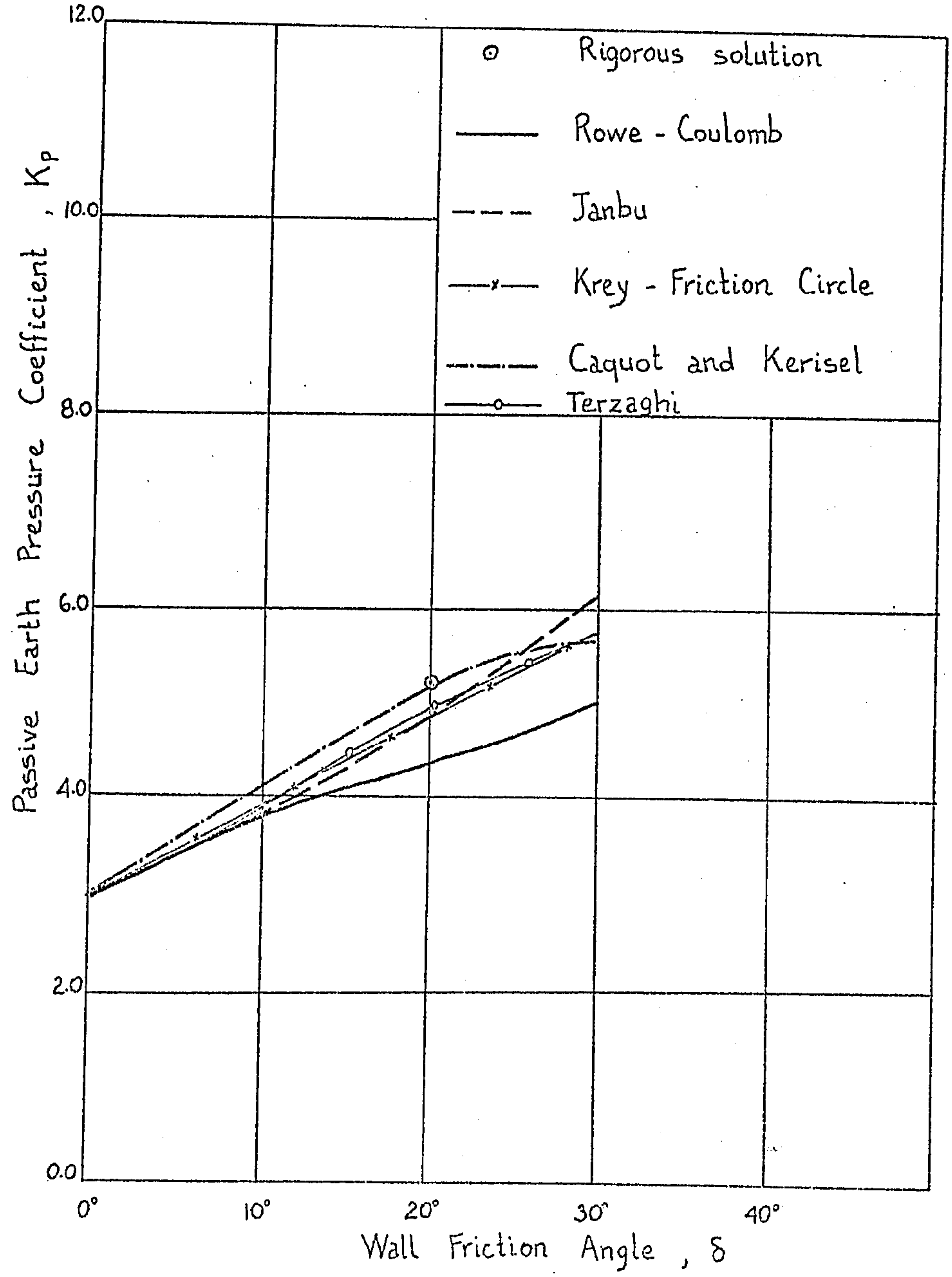

Figure 40. Comparison of Rowe-Coulomb values of K_p with other theories for $\phi'=30^{\circ}$.

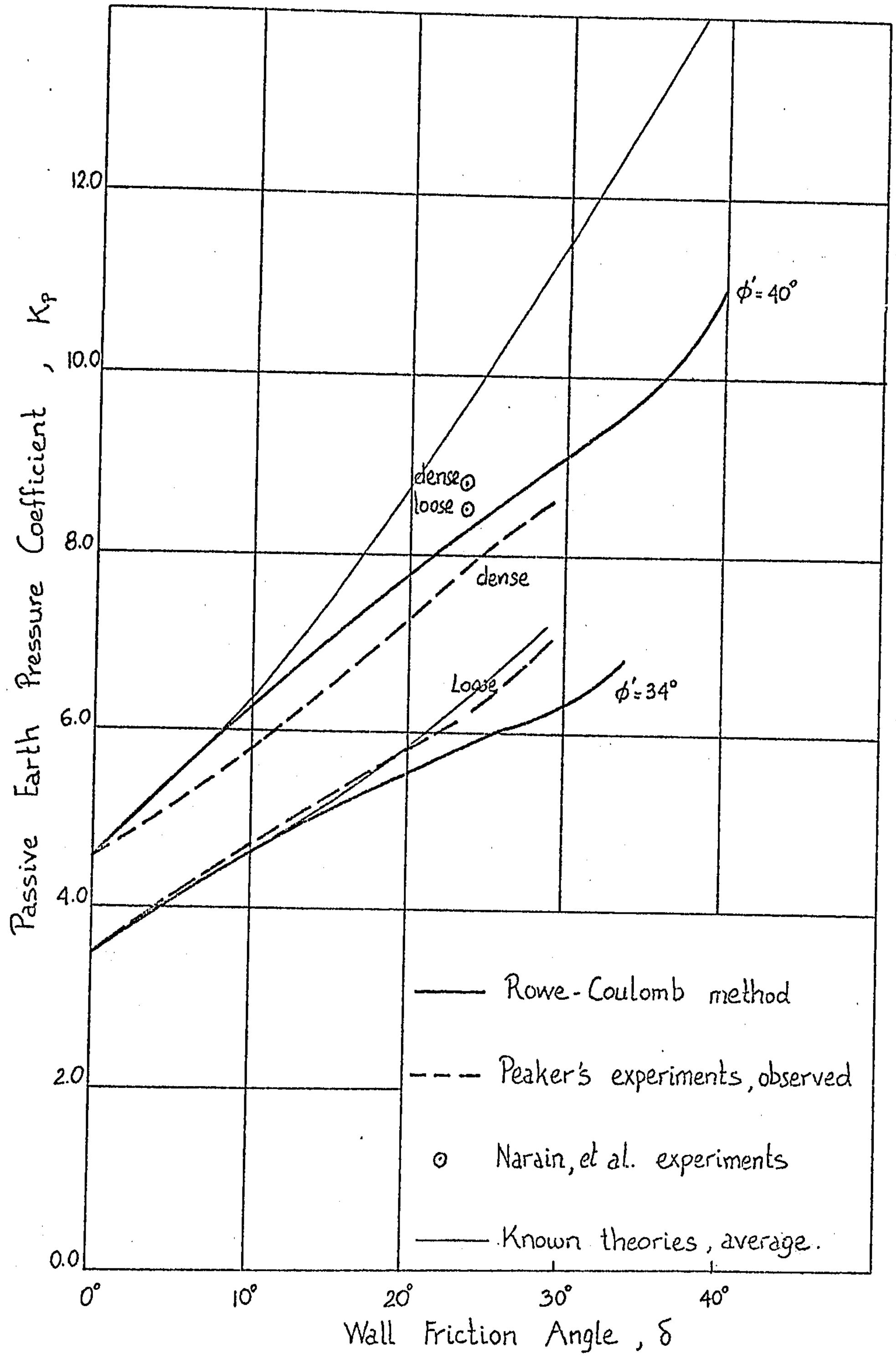

Figure 41. Comparison of K_p values obtained by the Rowe-Coulomb method with the experimental values of Peaker and of Narain, et al.

shear box results - $\phi'=41^{o}$ (dense)

$\phi'=34^{o}$ (loose)

δ determined by the shear box.

Narain et al. experiments,

$\phi'=38.5^{o}$ @ relative density of 31.5%

$\phi'=42.0^{o}$ @ relative density of 70.25%

$\delta=23.5^{o}$ (direct shear test)

From figure 41 it is seen that the values of K_p, calculated by using the Rowe-Coulomb method are slightly higher than the experimental values of Peaker for the dense sand ($\phi'=40^{o}$). Nevertheless, these values are the closest to the experimental results among all the known theories. The Rowe-Coulomb values for the loose sand ($\phi'=34^{o}$) are slightly lower than the experimental observations of Peaker. The low K_p values of Peaker for the dense sand could be a result of the mechanical vibrations given to the sand. Narain et al. give higher K_p values than the Rowe-Coulomb method.

v) Comparison of failure surfaces.

Failure surfaces obtained for the Rowe-Coulomb method and the experimental failure surfaces of Peaker for two cases are shown in figures 42 and 43. For the loose sand the Rowe-Coulomb method utilizes a failure surface fairly close to the findings of Peaker only at the wall and the sand surface. For the dense sand, while the shape of the predicted failure surface and the experimental surface are similar, the volumes of sand involved are very different. These can be explained by considering the velocity and stress fields (6,7).

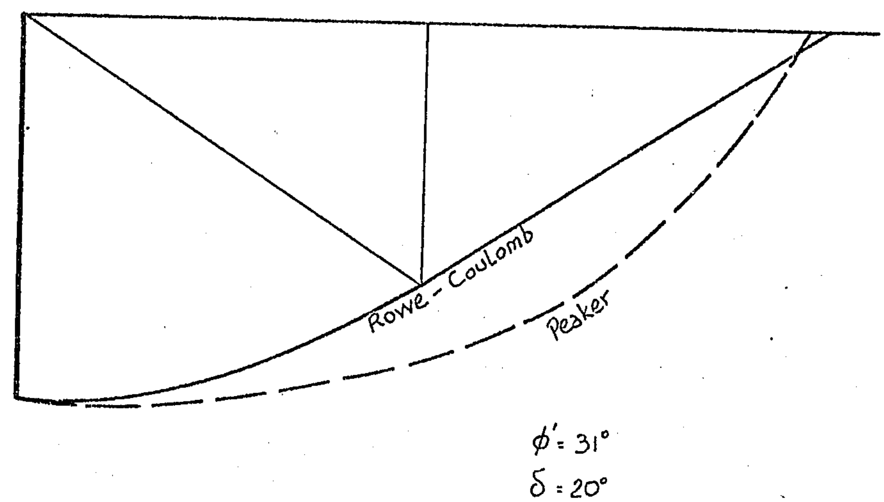

Figure 42. Comparison of failure surfaces for loose sand.

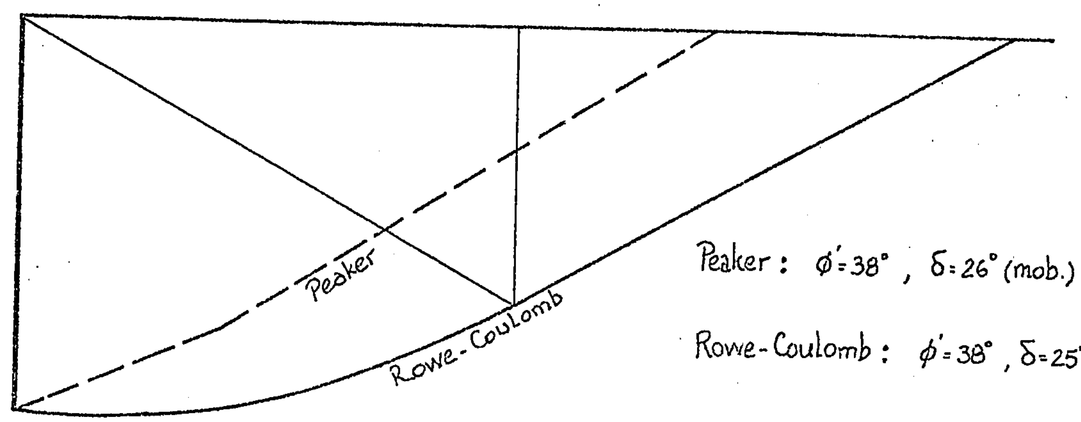

Figure 43. Comparison of failure surfaces for dense sand.

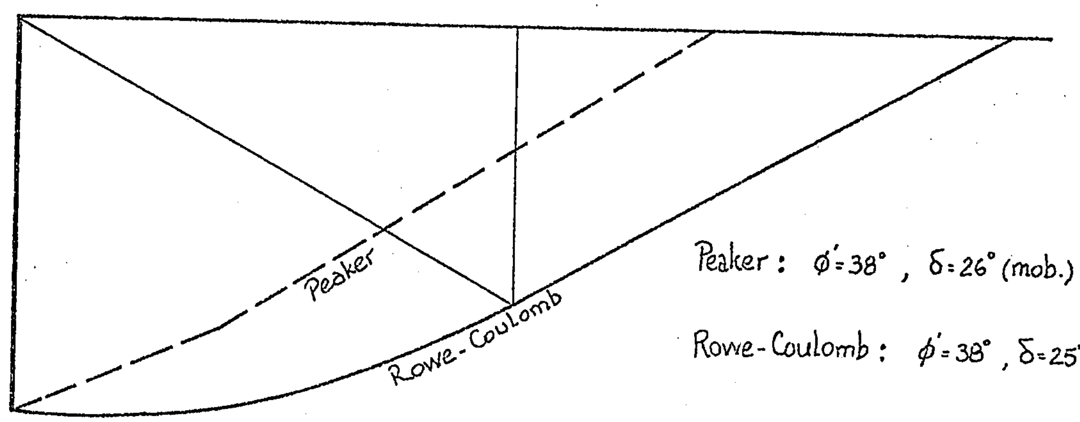

Figure 43. Comparison of failure surfaces for dense sand.

CHAPTER 8. CONCLUSION AND RECOMMENDATIONS FOR FURTHER WORK

i) The Rowe-Coulomb method is simple, convenient and meets the kinematic requirements of failure.

ii) K_p values obtained by the Rowe-Coulomb method are closer to the published experimental values than the values given by other theories currently available (dense).

iii) Because the other theories give higher K_p values than the Rowe-Coulomb method, this method is safer to use.

iv) The Rowe-Coulomb values are sufficiently close to the experimental values that they are recommended for design.

v) The assumption that all the shear is lost at the wall gives safer values for K_p. This finding parallels Bishop's simplification to the rigorous method of slices in slope stability work.

vi) K_p values are obtained for the special case of a dry, ideal sand against a vertical wall, with horizontal ground surface. The Rowe-Coulomb method can be extended to include inclined walls and sloping backfill. Cohesion and water pressure can also be introduced into the method to calculate K_p values for more general cases. It is also possible to investigate the effects of surcharge on the K_p values by introducing a surcharge force into the calculations.

vii) It would also be interesting to calculate the values of K_p using the Rowe-Coulomb method and applying it to different failure surfaces such as ellipses, circles etc., to see what influence the shape of the failure surface has on the theoretical values of K_p.

LIST OF REFERENCES

(1) BISHOP, A. W. 1955. 'The Use of Slip Circles in the Stability Analysis of Slopes'. Géotechnique, Vol. V.

(2) CAQUOT, A. and KERISEL, J. 1948. 'Tables for the Calculation of Passive Pressure, Active Pressures and Bearing Capacity of Foundations'. Gauthier-Villars, Paris.

(3) GRAHAM, J. 1968. 'Plane Plastic Failure in Cohesionless Soils'. Géotechnique 18.

(4) GRAHAM, J. 1971. 'Calculation of Passive Pressure in Sand'. Canadian Geotechnical Jour., Vol. 8, No. 4.

(5) HANSEN, B. 1952. 'Earth Pressure Calculations'. The Inst. of Danish Eng., Danish Tech. Press, Copenhagen.

(6) JAMES, R. G. and BRANSBY, P. L. 1970. 'Experimental and Theoretical Investigations of a Passive Earth Pressure Problem'. Géotechnique 20, No. 1.

(7) JAMES, R. G. and BRANSBY, P. L. 1971. 'A Velocity Field for some Passive Earth Pressure Problems'. Géotechnique 21, No. 1.

(8) JANBU, N. 1957. 'Earth Pressure and Bearing Capacity Calculations by Generalized Procedure of Slices'. Proc., 4th Intl. Conf. Soil Mechanics and

Foundation Engineering, Vol. II, London.

(9) JUMIKIS, A. R. 1962. 'Soil Mechanics'. D. Van Nostrand Comp., Inc., Princeton, N. J.

(10) JUMIKIS, A. R. 1962. 'Active and Passive Earth Pressure Coefficient Tables'. Engineering Research Publ., No. 43, Rutgers, The State University.

(11) NARAIN, J., SARAN, S. and NANDAKUMARAN, P. 1969. 'Model Study of Passive Pressure in Sand'. Proc., ASCE Jour. of the Soil Mechanics and Foundations Div., No. SM4.

(12) PACKSHAW, S. 1946. 'Earth Pressure and Earth Resistance'. A Century of Soil Mechanics, The Inst. of Civil Engineers, London, 1969.

(13) PEAKER, K. 1964. 'Passive Earth Pressure Measurements' PhD Thesis, University of Manchester, England.

(14) ROWE, P. W. 1963. 'Stress Dilatancy, Earth Pressures and Slopes'. Proc., ASCE Jour. of the Soil Mechanics and Foundations Div., Vol. 89, No. SM3.

(15) ROWE P. W. and PEAKER, K. 1965. 'Passive Earth Pressure Measurements'. Géotechnique, Vol. XV, No. 1.

(16) SCHOFIELD, A. N. 1961. 'The Development of Lateral Force of Sand Against the Vertical Face of a Rotating Model Foundation'. Proc., 5th Intl. Conf. Soil Mechanics and Foundation Engineering.

(17) SOKOLOVSKI, V. V. 1960. 'Statics of Soil Media'. Butterworths Scientific Publ., London.

(18) SUKLJE, L. 1969. 'Rheological Aspects of Soil Mechanics'. John Wiley & Sons Ltd.

(19) TAYLOR, D. W. 1948. 'Fundamentals of Soil Mechanics'. John Wiley & Sons Inc., New York, 6th printing.

(20) TCHENG, Y. and ABSI, E. 1969. 'Poussée et Butée en Vraie Grandeur'. Proc., 7th Intl. Conf. Soil Mechanics and Foundation Engineering, Mexico.

(21) TCHENG, Y. and ISEUX, J. 1971. 'Essais de Butée en Vraie Grandeur'. Annales de L'institut Tech. du Batiment et des Travaux Publics, Supplement au No. 281, Mai.

(22) TCHENG, Y. and ISEUX, J. 1971. 'Poussée-Butée'. Annales de L'institut Tech. du Batiment et des Travaux Publics, Supplement au No. 282, Juin.

(23) TERZAGHI, K. 1920. 'Old Earth Pressure Theories and New Test Results'. Engineering News-Record, Vol. 85, No. 14.

(24) TERZAGHI, K. 1954. 'Theoretical Soil Mechanics'. Wiley, 9th printing.

(25) TERZAGHI, K. and PECK, R. B. 1967. 'Soil Mechanics in Engineering Practice'. John Wiley & Sons Inc., 2nd edition.

(26) TSCHEBOTARIOFF, G. P. 1951. 'Soil Mechanics, Foundations, and Earth Structures'. McGraw-Hill Book Comp., Inc.

(27) VERDEYEN, J., ROISIN, V. and NUYENS, J. 1968. 'Mechanique des Sols'. Presses Universitaires de Bruxelles.

(28) WU, T. H. 1966. 'Soil Mechanics'. Allyn and Bacon, Inc., Boston.

APPENDIXES

APPENDIX A - KÖTTER'S EQUATION

Figure 44 shows the stresses acting on an infinitesimal soil element. The conditions of equilibrium in two dimensions will give the following relationships :

$\Sigma F_x = 0,$

$$\sigma_x dy - (\sigma_x + \frac{\partial \sigma_x}{\partial x} dx) dy + \tau_{xy} dy - (\tau_{xy} + \frac{\partial \tau_{xy}}{\partial y} dy) dy = 0$$

where $dx = dy$, therefore

$$\frac{\partial \sigma_x}{\partial x} + \frac{\partial \tau_{xy}}{\partial y} = 0 \qquad \text{(A.1)}$$

$\Sigma F_y = 0,$

$$\sigma_y dx - (\sigma_y + \frac{\partial \sigma_y}{\partial y} dy) dx + \tau_{xy} dx - (\tau_{xy} + \frac{\partial \tau_{xy}}{\partial x} dx) dx + \gamma . dx . dy = 0$$

then,

$$\frac{\partial \sigma_y}{\partial y} + \frac{\partial \tau_{xy}}{\partial x} = \gamma \qquad \text{(A.2)}$$

Condition of failure is expressed by the Mohr-

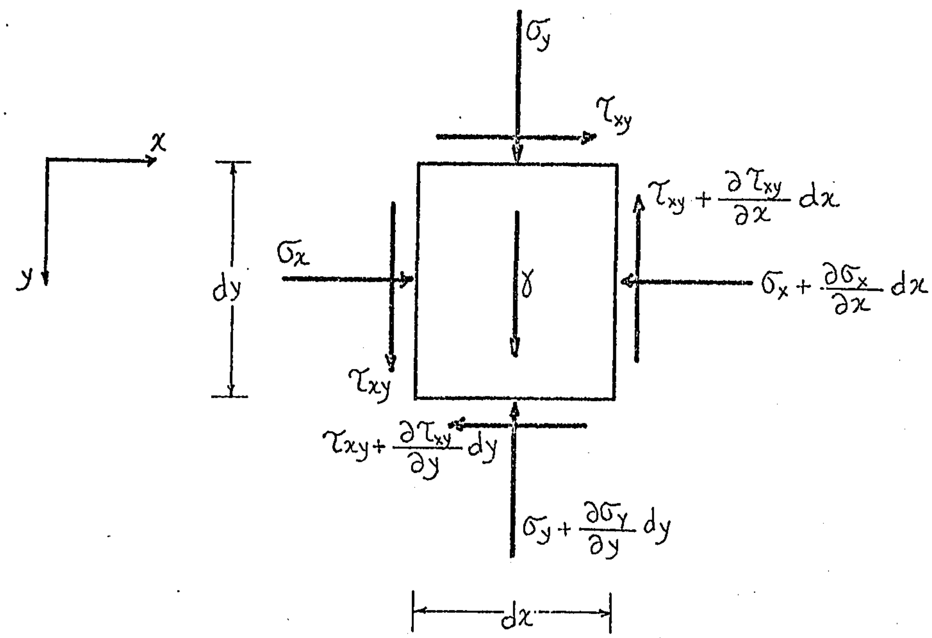

Figure 44. Stresses acting on an infinitesimal soil element.

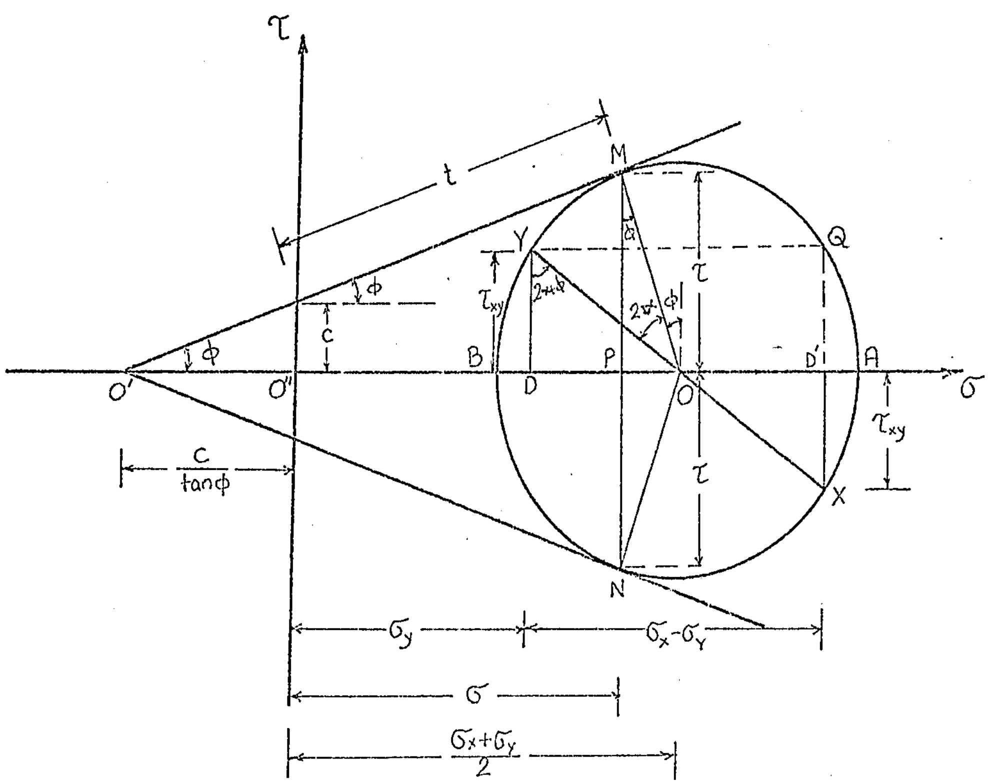

Figure 45. Mohr circle representation of the stresses.

Coulomb criterion :

$$\tau = c+\sigma\tan\phi \tag{A.3}$$

Equation (A.3) can be expressed in terms of σ_x, σ_y and τ_{xy} which are the stresses in any pair of orthogonal lines corresponding to points X and Y (figure 45).

From figure 45 :

$$(YQ)^2+(QX)^2 = (OY+OX)^2 = (2.OY)^2 = (2OM)^2$$

where,

$$YQ = \sigma_x - \sigma_y$$

$$QX = 2\tau_{xy}$$

$$OM = \frac{\tau}{\cos\phi} = \frac{c+\sigma\tan\phi}{\cos\phi} = \frac{c}{\cos\phi} + \frac{\sigma\sin\phi}{\cos^2\phi}$$

$$O'P = \sigma+\frac{c}{\tan\phi} = (O'M)\cos\phi$$

therefore,

$$\sigma = (O'M)\cos\phi - \frac{c}{\tan\phi}$$

$$O'M = \{\frac{\sigma_x+\sigma_y}{2} + \frac{c}{\tan\phi}\}\cos\phi$$

$$\sigma = \{\frac{\sigma_x+\sigma_y}{2} + \frac{c}{\tan\phi}\}\cos\phi.\cos\phi-\frac{c}{\tan\phi}$$

therefore,

$$OM = \frac{c}{\cos\phi} + \frac{\{[\frac{\sigma_x+\sigma_y}{2} + \frac{c}{\tan\phi}]\cos^2\phi-\frac{c}{\tan\phi}\}\sin\phi}{\cos^2\phi}$$

after simplifications,

$$OM = \tfrac{1}{2}(\sigma_x+\sigma_y)\sin\phi+c.\cos\phi$$

but $$(YQ)^2+(QX)^2 = 4(OM)^2$$

therefore,

$$(\sigma_x-\sigma_y)^2+4\tau_{xy}^2 = \{(\sigma_x+\sigma_y)\sin\phi+2c.\cos\phi\}^2 \qquad (A.4)$$

The three stresses σ_x, σ_y, and τ_{xy} can be determined with the three equations (A.1), (A.2) and (A.4). Instead of the three unknown stresses two other variables t and α may be introduced where,

$$t = \sigma\sec\phi$$

and

α = angle between the rupture line and the horizontal.

$$\sigma_x = O''O+OD' = O''O+OD$$

where,

$$OD = (OY)\sin(2\alpha+\phi)$$

$$OY = OM = \frac{c+t.\sin\phi}{\cos\phi} = c.\sec\phi+t.\tan\phi$$

then,

$$OD = (c.\sec\phi+t.\tan\phi)\sin(2\alpha+\phi)$$

also,

$$O''O = O''P+OP$$

where,

$$OP = (OM)\sin\phi = (c.\sec\phi+t.\tan\phi)\sin\phi$$

$$O''P = t.\cos\phi$$

therefore,

$$O''O = t.\cos\phi+(c.\sec\phi+t.\tan\phi)\sin\phi = t.\sec\phi+c.\tan\phi$$

Combining these expressions :

$$\sigma_x = (t.\sec\phi+c.\tan\phi)+(t.\tan\phi+c.\sec\phi)\sin(2\alpha+\phi) \qquad (A.5)$$

On the other hand,

$$\sigma_y = O''O - OD$$

therefore,

$$\sigma_y = (t.\sec\phi + c.\tan\phi) - (t.\tan\phi + c.\sec\phi)\sin(2\alpha + \phi) \qquad \text{(A.6)}$$

From triangle DOY :

$$\tau_{xy} = (OY)\cos(2\alpha + \phi)$$

therefore,

$$\tau_{xy} = (t.\tan\phi + c.\sec\phi)\cos(2\alpha + \phi) \qquad \text{(A.7)}$$

For the determination of t and α we have the equations (A.1) and (A.2) as equations (A.5), (A.6) and (A.7) satisfy the equation (A.4). By different transformations the following equation may be derived :

$$\frac{\partial t}{\partial s} + 2(t.\tan\phi + c.\sec\phi)\frac{\partial \alpha}{\partial s} + \gamma \sin(\alpha + \phi) = 0 \qquad \text{(A.8)}$$

where s is the arc length of the rupture line in question.

In the case of the cohesionless soil where c=0, equation (A.8) is reduced to :

$$\frac{\partial t}{\partial s} + 2t.\tan\phi \frac{\partial \alpha}{\partial s} + \gamma \sin(\alpha+\phi) = 0 \qquad (A.9)$$

Equation (A.9) is known as Kötter's equation.

APPENDIX B - TERZAGHI'S METHOD

"Since the methods for determining the real shape of the surface of sliding are not suitable for practical purposes, the sufficiently accurate method of assuming this surface to be composed of a logarithmic spiral and a straight line is used" (25). The logarithmic spiral has the equation :

$$r = r_o e^{\theta \tan\phi} \qquad (5.3)$$

The soil behind the retaining wall AB is assumed to be non-cohesive, dry, ideal and the resultant force is assumed to be acting at the lower third point. This method can also be applied to a case where there is cohesion.

The failure surface and the forces acting on it are shown in figure 46. Since the logarithmic spiral is tangent at point D to the straight line part DE of the surface of sliding, the center O of the spiral must be located on the line AD which is inclined at $(45^o - \frac{1}{2}\phi)$ to the horizontal. According to the equation of the logarithmic spiral every radius vector makes an angle of ϕ with the normal to the spiral at the point where it intersects the failure surface. Since ϕ is the angle of internal friction the resultant of the normal stress and the frictional resistance on any

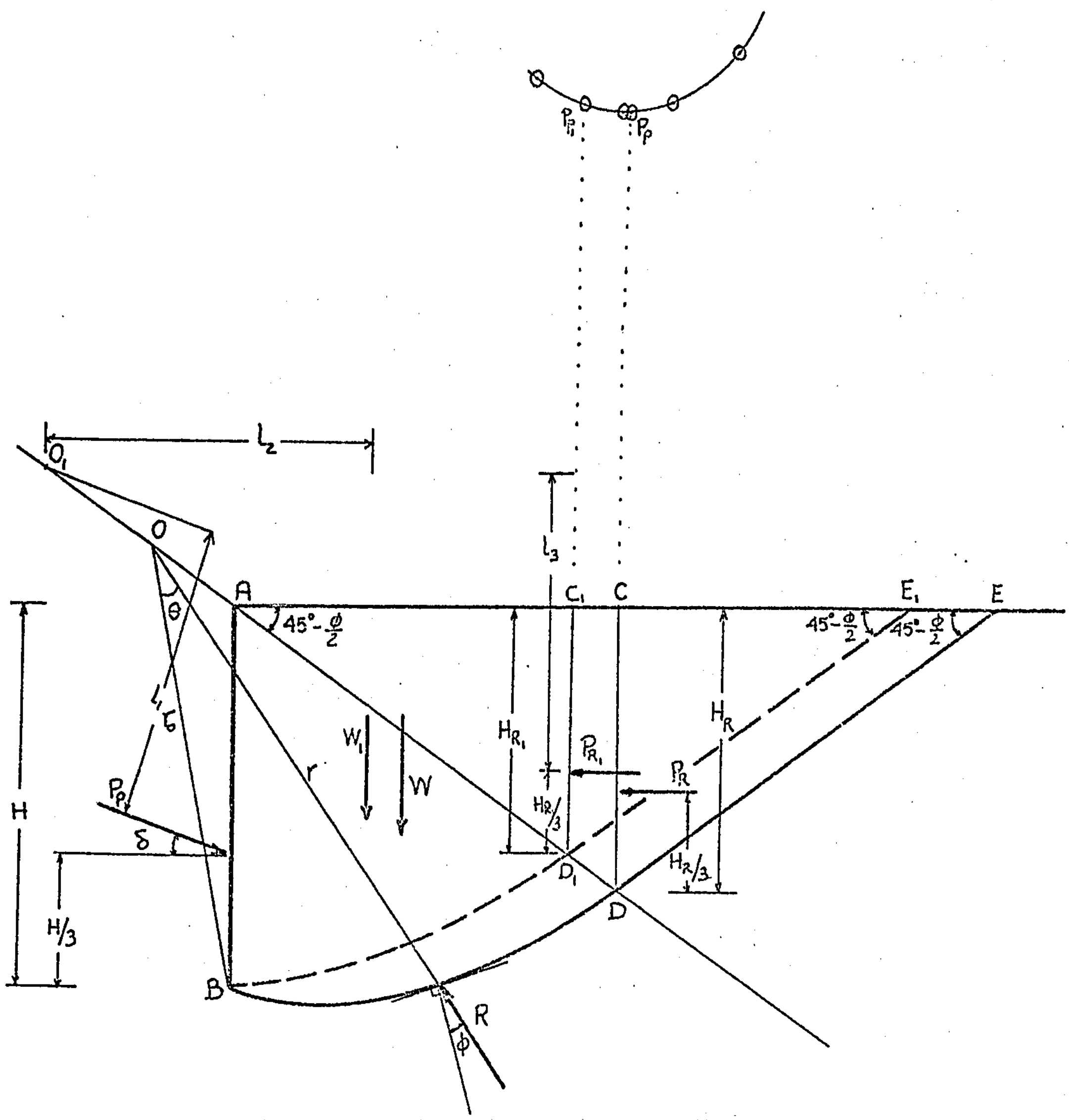

Figure 46. Terzaghi's method of finding the passive earth pressure for a cohesionless soil.

element of the surface of sliding also makes an angle of ϕ with the normal to the element and its direction coincides with that of the radius vector subtending the element. Every radius vector of the logarithmic spiral has to pass through point O, therefore the resultant R of the normal and frictional forces on BD also pass through the center O.

In order to calculate P_p an arbitrary surface of sliding, BD_1E_1 is selected. The part BD_1 is a logarithmic spiral with its center at O_1 and the straight line D_1E_1 makes an angle of $(45^{\circ}-\frac{1}{2}\phi)$ with the horizontal. The forces acting on the area ABD_1C_1 are then considered and the moments of these forces about the point O_1 are taken. The force P_{R_1} exerted by the portion $D_1E_1C_1$ which is in a Rankine state is given by :

$$P_{R_1} = \tfrac{1}{2}\gamma H_{R_1}^2 \tan^2(45^{\circ}+\tfrac{1}{2}\phi)$$

The moment of R_1 about point O_1 is zero and therefore the moment equilibrium equation is :

$$P_{p_1} l_1 = W_1 l_2 + P_{R_1} l_3$$

from which,

$$P_{p_1} = \frac{W_1 l_2 + P_{R_1} l_3}{l_1}$$

The value P_{p_1} is plotted to scale above the point C_1 and similar computations are performed for other arbitrary surfaces of sliding. A curve is then passed through the points obtained. Values of the passive earth pressure coefficient K_p for the horizontal component may be calculated from the relation :

$$P_p \cos\delta = \tfrac{1}{2}\gamma H^2 K_p$$

and plotted instead of the P_p values. The minimum ordinate of the curve will give the required value of K_p. The failure surface will pass through the point located on AD (or its extension) vertically below the minimum ordinate of the curve.

Results of the calculations for the case where ($\phi=30^o$, $\delta=30^o$) are shown in figure 47. In these calculations H is taken to be 10 feet. The values given are for the resultant force and therefore have to be multiplied by $\cos\delta=0.866$ in order to get K_p.

Values of K_p calculated, using Terzaghi's method, are given in figure 48.

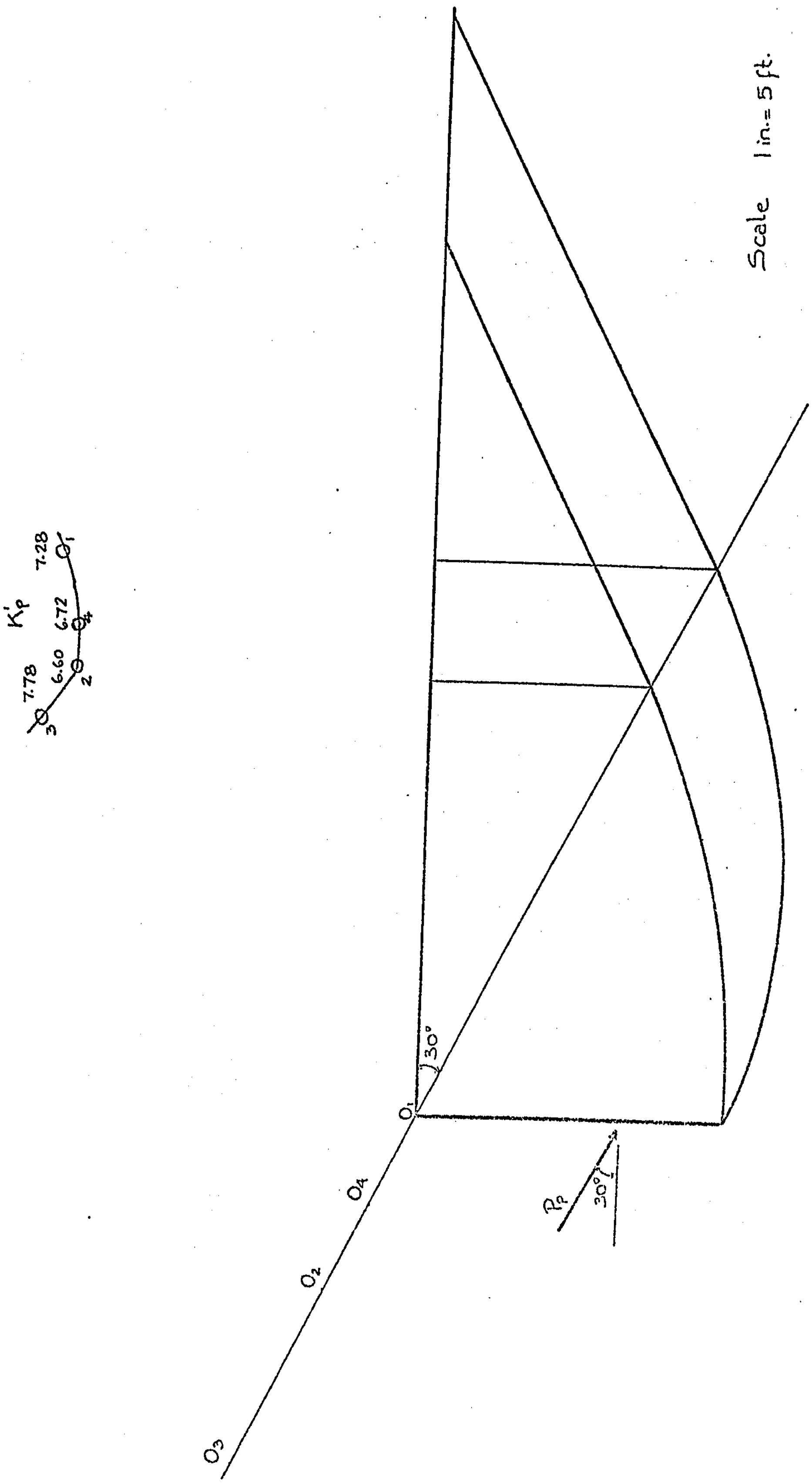

Figure 47. K_p calculations using Terzaghi's method ($\phi=\delta=30^{\circ}$)

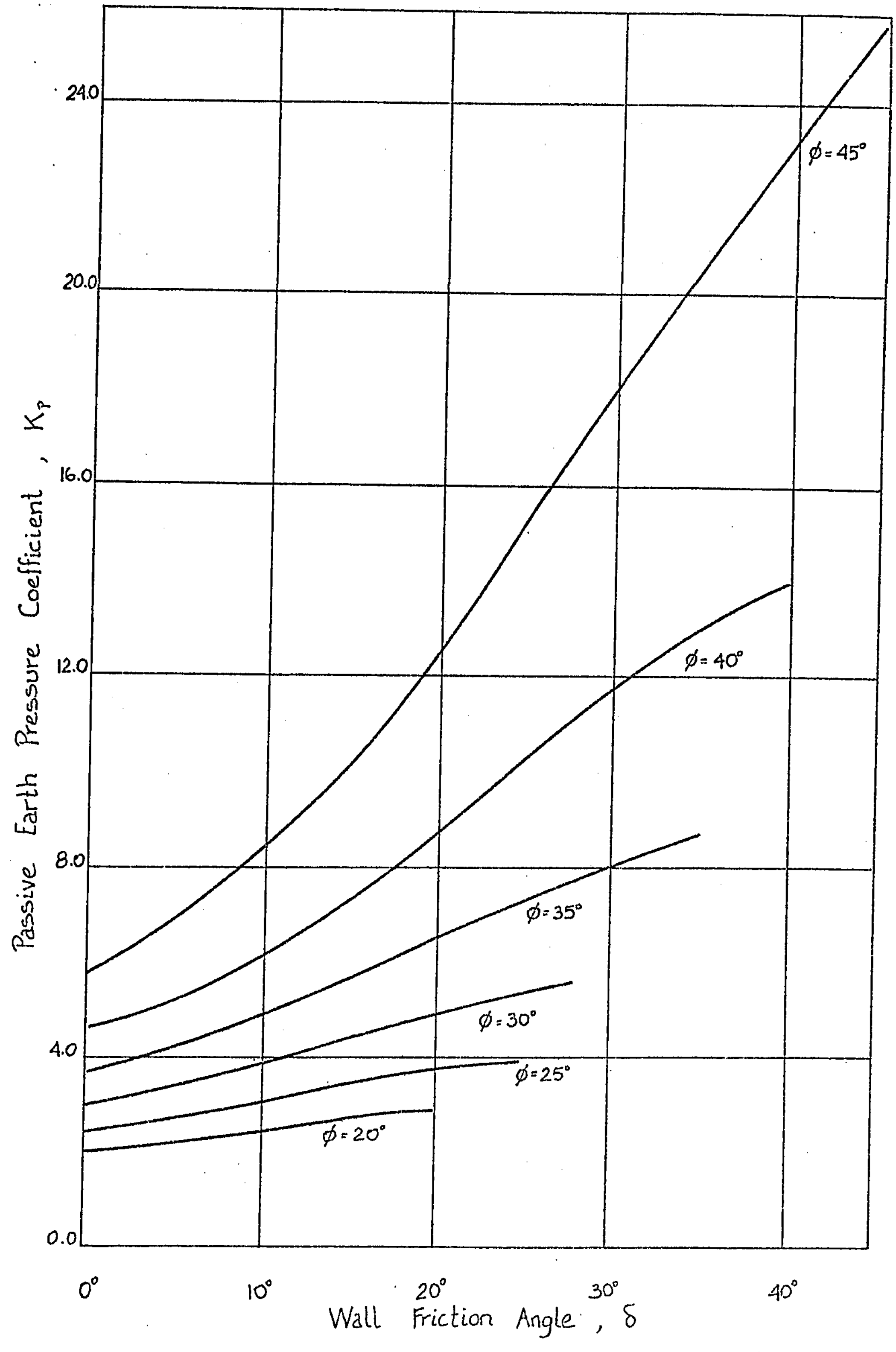

Figure 48. K_p values for dry, cohesionless sand with a horizontal surface acting against a vertical, rough wall - Terzaghi's method.

APPENDIX C - ADDITIONAL REFERENCES

(1) COULOMB, C. A. 1776. 'Essai sur une Application des Règles Maximis et Minimis à Quelques Problèmes de Statique Relatifs à L'Architecture'. Mem. Div. Sav. Acad. des Science, Vol. 7.

(2) CULMANN, K. 1866. 'Die Graphische Statik'. Meyer and Zeller, Zurich.

(3) FRANZIUS, O. 1924. 'Experiments with Passive Earth Pressure'. Bauing.

(4) FRANZIUS, O. 1928. 'Earth Pressure Measurements on a Natural Scale'. Bauing.

(5) KÉZDI, A. 1962. 'Earth Pressure Theories'. Proc., Lec. Series, Design of Structures to Resist Earth Pressures, Chicago.

(6) KÖTTER, F. 1903. 'Die Bestimmung des Druckes an Gekrümmten Gleitflächen'. Sitzungsber. Kgl. Preuss. Akad. des Wiess., Berlin.

(7) KREY, H. 1936. 'Erddruck Erdwiderstand'. 5th edition, Berlin.

(8) LAMBE, T. W. and WHITMAN, R. V. 1969. 'Soil Mechanics'. John Wiley & Sons, Inc.

(9) LEE, I. K. and MOORE, P. J. 1968. 'Stability Analyses Application to Slopes, Rigid and Flexible Retaining Structures'. Selected Topics in Soil

Mechanics, Edited by I. K. Lee, Butterworth and Co. Ltd.

(10) OHDE, J. 1938. 'Zur Theories des Erddruckes Unter Besonderer Berüchsichtigung des Erddruck Verteilung die Bautechnik'. Vol. 16.

(11) PONCELET, J. V. 1840. 'Memoire sur la Stabilite des Revêtments et de leurs Fondation'. Memorial de L' Officier du Genie, Vol. 13, Paris.

(12) RANKINE, W. J. M. 1857. 'On the Stability of Loose Earth'. Phil. Trans. Royal Soc., Vol. 147, London.

(13) ROWE, P. W. 1952. 'Anchored Sheet Walls'. Proc. Inst. of Civil Eng., Part 1.

(14) ROWE, P. W. 1954. 'A Stress Strain Theory for Cohesionless Soils with Application to Earth Pressure at Rest and Moving Walls'. Géotechnique, Vol. IV.

(15) ROWE, P. W. 1961. 'The Stress-Dilatancy Relation for Static Equilibrium of an Assembly of Particles in Contact'. Proc. Royal Soc., Series A, Vol. 269.

(16) TSCHEBOTARIOFF, G. P. and JOHNSON, E. G. 1953. 'Report to U. S. Navy'. Princeton Univ.

(17) TSCHEBOTARIOFF, G. P. 1962. 'Retaining Structures'. Foundation Engineering, Edited by G. A. Leonards, McGraw-Hill Book Co.

RESUME

The publishing of Charles Augustin Coulomb's work " Essai sur une application des règles de maximus et minimis à quelques problèmes de statique relatifs à l'architecture " in 1776 marked the first rigorous analysis of the lateral earth pressure problem. Coulomb's consideration of a sliding wedge behind a wall for the active (wall yielding away from the backfill) and for the passive (wall pushing against the backfill) cases gives useful results agreeing with the experimental values for the lateral pressures with no wall friction, ie. smooth wall. On the other hand his results differ considerably from reality when applied to a rough wall with the backfill in a passive state.

Following this work other analyses were introduced by various authors, such as : W. Rankine, H. Krey, J. Ohde, K. Terzaghi, A. Caquot, Brinch Hansen, V. Sokolovski, N. Janbü and P. Rowe, in order to estimate the lateral earth pressures on structures.

The principal contribution of the more recent workers was to alter the plane shape of Coulomb's failure wedge into the shape of a curved surface when there was wall friction present. Different authors used different shapes for this curved surface and calculated the lateral pressures accordingly. These studies showed that there was no appreci-

able disagreement between the values computed for the active case and the Coulomb's values, but the passive pressure values differed appreciably from Coulomb's calculations, in agreement with the experimental findings.

A careful experimental study of the passive earth pressure case for sands was carried out by K. Peaker in 1964 at the University of Manchester under professor P. Rowe. A rough wall gave values of passive earth pressure coefficients (ratio of the horizontal force to the vertical force at the wall, when the wall pushes towards the backfill) lower than the theoretical values available at that time. Since for many structures the passive earth pressure is relied upon at least partially for stability, Peaker's results were very disturbing. All existing theories gave predictions which were unsafe for rough walls.

Although Rowe had worked out a theory for the earth pressure problem using the method of slices commonly employed in slope stability work, only a limited number of calculations appears to have been made and no comparison was made with Peaker's results. In fact Rowe's theory is as yet unpublished except for a brief reference to the method in " Selected Topics in Soil Mechanics " edited by I. K. Lee. It is this method that is used in this study of the particular problem of a rough, vertical wall pushing into a cohesionless, dry backfill with a horizontal ground surface.

Passive earth pressure coefficients, K_p, based on

Rowe's method are presented for angles of internal friction, ϕ', varying from 20 degrees to 45 degrees (representing loose to dense sand) and for wall friction angles, δ, of zero degrees to ϕ' degrees (representing smooth to rough walls). These results are consistantly lower than those of previous theories and are quite close to the experimental values found by Peaker.